



universität  
wien

# DIPLOMARBEIT

Titel der Diplomarbeit

Characterization of the inversion reaction of  $\phi$ Ch1  
and  
the establishment of a transformation system for *Natrialba magadii*

angestrebter akademischer Grad

Magistra der Naturwissenschaften (Mag. rer.nat.)

Verfasserin / Verfasser:	Angela Ladurner
Matrikel-Nummer:	0201490
Studienrichtung (lt. Studienblatt):	Molekulare Biologie (A490)
Betreuerin / Betreuer:	Ao. Prof. Dr. Angela Witte

Wien, im Mai 2008

---

---

---

---

# Table of Contents

<b>1. INTRODUCTION</b>	<b>9</b>
1.1. Archaea	9
1.2. Halophilic Archaea	10
1.3. Archaeal viruses	12
1.4. Virus $\phi$ Ch1 and its host <i>Natrialba magadii</i>	15
1.4.1. <i>Nab. magadii</i>	15
1.4.1. General aspects of $\phi$ Ch1	16
1.4.2. Origin of replication of $\phi$ Ch1	19
1.4.3. Some aspects about gene regulation in $\phi$ Ch1	20
1.5. Site-specific recombination	21
<b>2. MATERIALS AND METHODS</b>	<b>27</b>
2.1. Methods	27
2.1.1. Archaeal strains	27
2.1.2. Bacterial strains	28
2.1.3. Plasmids	28
2.1.4. DNA marker	31
2.1.5. Protein marker	31
2.1.6. Primer	31
2.1.7. Restriction enzymes and buffers	33
2.1.8. Media	33
2.1.9. Antibiotics – stock solutions	35
2.1.10. Antibodies	36
2.1.11. General buffers and solutions	36
2.2. Methods	41

---

2.2.1. <i>E. coli</i> methods	41
2.2.1.1. MOPS competent cells	41
2.2.1.2. Transformation of MOPS competent cells	41
2.2.2. <i>Archaeal</i> methods	42
2.2.2.1. Phage titers	42
2.2.2.2. Transformation of halophilic and haloalkaliphilic archaea	42
2.2.2.3. Isolation of plasmid DNA from halo(alkali)philic <i>Archaea</i> and retransformation	43
2.2.2.4. Plasmid copy number determination	43
2.2.3. DNA methods	43
2.2.3.1. Polymerase chain reaction	43
2.2.3.2. Purification of PCR and DNA fragments	44
2.2.3.3. Restriction of DNA	44
2.2.3.4. Ligation of DNA	45
2.2.3.5. Plasmid preparation	45
2.2.3.6. Agarose gel electrophoresis	46
2.2.3.7. Southern blot	46
2.2.4. Protein methods	48
2.2.4.1. Overexpression of proteins in <i>E. coli</i>	48
2.2.4.2. Expression of proteins in <i>Nab. magadii</i>	49
2.2.4.3. SDS PAGE (Laemmli system)	49
<b>2.3. Cloning strategies</b>	<b>52</b>
2.3.1. Construction of plasmids containing different fragments of the putative origin region of $\phi$ Ch1	52
2.3.2. Construction of plasmids to analyse the function of the $\lambda$ -like integrase Int1	54
<b>3. RESULTS AND DISCUSSION</b>	<b>57</b>
<b>3.1. Establishment of a shuttle vector system for <i>Natrialba magadii</i></b>	<b>57</b>
3.1.1. Development and analysis of different vectors	57
3.1.2. Characterization of <i>Nab. magadii</i> transformants	67

---

3.1.3. Transformation of different halophile and haloalkaliphile <i>Archaea</i>	71
<b>3.2. The influence of Int1 in the inversion reaction of <math>\phi</math>Ch1</b>	<b>74</b>
3.2.1. Analysis of single repeat constructs in <i>E. coli</i>	74
3.2.2. Analysis of multiple repeat constructs in <i>E. coli</i>	76
3.2.3. Analysis of Int1 in <i>Nab. magadii</i>	80
<b>4. INDEX OF FIGURES AND TABLES</b>	<b>84</b>
<b>5. REFERENCES</b>	<b>91</b>
<b>Acknowledgements</b>	<b>98</b>
<b>Zusammenfassung</b>	<b>99</b>
<b>Abstract</b>	<b>101</b>
<b>Curriculum vitae</b>	<b>103</b>

---



---

# 1. Introduction

## 1.1. *Archaea*

Until 1977 the scientific world knew only about two domains of life: the prokaryotes and the eukaryotes. In 1977 Carl Woese and George Fox discovered three classes of ribosomal RNA and ribosomes by molecular analyses of the 16S rRNA sequence. With Woese's work a third domain was added, the domain of the *Archaea* (Woese and Fox, 1977).

*Archaea* have different features from both of the two other domains. They resemble *Bacteria* concerning their cellular ultrastructure and genome organization, as they don't have e.g. cell organelles and a cytoskeleton but they have covalently closed circular chromosomes. *Archaea* share basic similarities with eukaryotes in DNA replication, transcription and translation machinery. *E.g.* the RNA polymerase is composed of much more subunits than the bacterial one, and in protein synthesis the initiator tRNA is not like in prokaryotes formyl-methionine but an unmodified methionine like in eukaryotes. However *Archaea* also have features exclusive for them. The cell walls of *Archaea* contain no peptidoglycan what disconnects them from *Bacteria*. Archaeal cell walls can consist of several different chemical compounds like the bacterial-like pseudopeptidoglycan, but also polysaccharides, proteins and glycoproteins but eukaryotic cell walls are usually made of cellulose or chitin. Another unique feature of *Archaea* is the assembly of membrane lipids. In *Bacteria* and *Eukarya* the linkage between hydrocarbons and glycerol is an ester linkage that leads to the formation of linear fatty acid molecules. In *Archaea* this connection is formed by an ether linkage that leads to the formation of long and branched fatty acid molecules (Brown and Doolittle, 1997).

The domain *Archaea* is divided into three kingdoms: the *Crenarchaeota*, the *Euryarchaeota* and the *Korarchaeota* (Woese *et al.*, 1990). The *Crenarchaeota* contain species living in hyperthermal environments up to 100°C as well as in deep sea environments with temperatures around the freezing point. These species are

---

obligate anaerobes with only a few exceptions and live chemotrophic using either organic or anorganic compounds as energy source. The *Euryarchaeota* contain methanogens, extreme halophiles as well as a few hyperthermophile species including the cell wall-less *Thermoplasma*. *Korarchaeota* are the latest kingdom added. They were discovered by 16S rRNA sequence analysis of a sample from a neutral pH hot spring (Barns *et al.*, 1996).

All of the three kingdoms contain species living in very extreme environments. This fact raised the interest of biotechnology in *Archaea* as their enzymes are still active under these extreme conditions. The best known examples for extremozymes are DNA polymerases used for polymerase chain reactions (PCR) like *Pfu*-DNA Polymerase from *Pyrococcus furiosus* and *Pwo*-DNA Polymerase from *Pyrococcus woesei* (Satyanarayana *et al.*, 2005).

## **1.2. Halophilic Archaea**

Halophilic *Archaea* are part of the family *Halobacteriaceae* in the kingdom of the *Euryarchaeota* and were first isolated from hides and salted fish. Members of this family are for example *Halobacterium* and *Haloferax* but also haloalkaliphilic genera like *Natronobacterium* and *Natrialba*, that need pH values from 9 to 11 for optimal growth. Halophilic *Archaea* occur in highly saline environments with a minimum salt concentration of 1.5 M NaCl (9%) and with an optimum from 2 to 4 M NaCl (12-23%). Most of the extreme saline environments are in hot and dry areas. Examples are the Great Salt Lake in Utah that composes of concentrated seawater, or the Soda Lake Magadi in Kenya. Except of halophilic *Archaea* eukaryotic and oxygenic phototroph algae are found in salt lakes. Anoxygenic phototrophic purple bacteria are found in soda lakes with pH values from 9 to 11. These organisms produce the organic compounds necessary for the growth of these chemoorganotrophic halophilic *Archaea* (Grant and Larsen, 1989).

Halophilic *Archaea* have to adapt their water balance to the high salt concentrations in their environment. Therefore they preserve a relatively high

---

potassium concentration inside the cells through different transporter systems that transport potassium, chloride and nutrients in and sodium out of the cells. Potassium is required in halophilic *Archaea* to maintain *e.g.* the activity of several enzymes like dehydrogenases (Jolley *et al.*, 1997; Madern *et al.*, 1995).

The outermost layer of haloarchaeal cells consists of a paracrystalline protein surface layer, the so-called S-layer (Figure 1). S-layers form a regularly ordered planar array of proteinaceous subunits. These glycoproteins consist with a high proportion of the negatively charged amino acids aspartate and glutamate. N-glycosylation sites can also introduce negative charges because each glucuronic acid is sulfated at its 3' position. These negative charges are neutralized by the binding of sodium ions and in some cases with the binding of bivalent cations like magnesium. Dilution of the environmental composition for example through rain leads to lysis of cells, because stabilizing cations are absent. The S-layer anchors fix the cell shape in situations of water influx and the diameter of the cells remains stable.

S-layers can have very different features *e.g.* lattice symmetry and the size of the unit cell. These features can be altered at the genome level by environmental factors and are not determined for a species.

S-layers don't have a common function but many advantageous roles. They can act as protective coats, as structures involved in cell adhesion and surface recognition, as molecular sieves and traps and as virulence factors (Engelhardt, 2007a and 2007b; Sleytr and Beveridge, 1999).

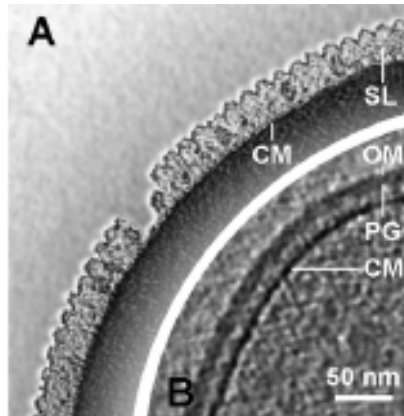


**Figure 1: Cell envelopes of an archaeon and a Gram-negative bacterium in a near-to-life state as obtained by cryo-electron tomography. (A) Section through the tomogram of an ice-embedded cell of *Pyrodictium abyssi*. The S-layer (SL) is anchored via long stalks in the cell membrane (CM) and defines the quasi-periplasmic space of the cell wall. The cytoplasmic density is removed. (B) A corresponding tomographic section through an ice-embedded cell of *Escherichia coli*, showing the cell envelope with the cell membrane (CM), the peptidoglycan (PG) and the outer membrane (OM). Note the considerable distance between the cell membrane and the peptidoglycan (Engelhardt, 2007).**

### **1.3. Archaeal viruses**

The development of transformation and shuttle vector systems for Archaea is strongly associated with archaeal viruses. They can be a tool to the successful transformation of different archaeal species.

The first two isolated archaeal viruses resembled members of the family Myoviridae. Icosahedral heads, contractile helical tails and a linear dsDNA genome were three features that these viruses shared for example with the bacteriophage T4 (Torsvik and Dundas, 1974; Wais *et al.*, 1975). Later on it was discovered that head-tail viruses are very rare among archaeal viruses (Dyall-Smith *et al.*, 2003; Prangishvili, 2003). Many different families of viruses are known until now and were categorised by means of their morphology.

---

Fusiform viruses are viruses with exceptional morphologies exclusive and common within *Archaea*. Like the *Sulfolobus* spindle-shaped viruses SSV1 and SSV2, and the *Acidianus* two-tailed virus (ATV), where the tails consist of tubes, which terminate in an anchor-like structure (Prangishvili *et al.*, 2006; Stedman *et al.*, 2003). They have a huge host range including hyperthermophile, extremely halophilic and methanogenic species (Rachel *et al.*, 2002; Oren *et al.*, 1997). Most of them have circular genomes and are able to integrate into the host genome by the action of an integrase (Muskhelishvili *et al.*, 1993). Fusiform viruses contain three families, the *Fuselloviridae*, the *Bicaudaviridae* and the *Salterporvirus* genus. Bottle-shaped and droplet-shaped viruses are so unique in terms of their morphology that they were assigned to new families. The *Acidianus* bottle-shaped virus (ABV) infects the hyperthermophile species *Acidianus* and was assigned to the family *Ampullaviridae* (Haring *et al.*, 2005). The *Sulfolobus neozealandicus* droplet-shaped virus (SNDV) infects the hyperthermophile species *Sulfolobus* and is the sole member of the family *Guttaviridae* (Arnold *et al.*, 2000).

The main virions in terrestrial hot environments above 80°C are linear viruses. They were separated into two families in respect to their morphology. The family of the *Rudiviridae* possess a stiff, rod-like appearance and the family of the *Lipothrixviridae* have a flexible, filamentous shape (Prangishvili *et al.*, 2006). Members of these families are predominantly *crenarchaea* from the genera *Sulfolobus*, *Acidianus* and *Thermoproteus* (Rachel *et al.*, 2002; Rice *et al.*, 2001). Linear archaeal viruses don't integrate into the host genome and therefore lack an integrase gene. They persist stably in the host cells and replication of viral genes is not induced upon stress factors like UV irradiation or mytomycin C treatment (Prangishvili *et al.*, 2006). There is only one exception of a lytic lipothrixvirus *Thermoproteus tenax* virus 1 (TTV1) of the neutrophilic hyperthermophile genus *Thermoproteus* (Janekovic *et al.*, 1983).

A remarkable feature was found in a member of the *Lipothrixviridae*. The multiple repeat pattern at the termini of the genome of the lipothrixvirus AFV1 resembles the telomeric ends of the linear chromosomes of eukaryotes (Bettstetter *et al.*, 2003).

---

Spherical viruses within the family of the *Globuloviridae* can also be found among archaeal viruses (Prangishvili *et al.*, 2006).

Head-tail viruses with non-enveloped virions were the first archaeal viruses isolated and carry icosahedral heads and helical tails. They are all associated with the kingdom *Euryarchaeota* and infect exclusively extreme halophiles and methanogens that are either mesophilic or moderately thermophilic. They have linear dsDNA genomes and are members of the families *Myoviridae* and *Siphoviridae* (Dyall-Smith *et al.*, 2003). Archaeal head-tail viruses resemble dsDNA bacteriophages in their genome content and in possessing mosaic genomes that have undergone extensive genetic exchange (Hendrix *et al.*, 1999; Pedulla *et al.*, 2003).

The high similarity in the gene content of viral species from the same family that are separated by large geographical distances is in contrast to the minimal similarity observed for species from different families that coexist in the same local microbial community (Prangishvili *et al.*, 2006).

A very interesting and unsolved question is the origin and evolution of viruses. Many different hypotheses are common. Viruses may have originated in a pre-cellular world, may be a reduction of parasitic cells, or may have originated from fragments of cellular genetic material that escaped from cellular control and became parasitic (Prangishvili *et al.*, 2006). The hypothesis of a last universal cellular ancestor (LUCA) states that this organism had an ancient virosphere from which all other viruses have developed and separated into three different types: bacterial, archaeal and eukaryotic viruses (Bamford *et al.*, 2005; Forterre, 2006).

96% of bacterial viruses are non-enveloped head-tail bacteriophages from the order *Caudovirales* (Fauquet *et al.*, 2005). Archaeal viruses especially in hot environments are very diverse and head-tail viruses are rather rare. Maybe this diversity was once common in all environments but was reduced by successful expansion of bacteria and their phages in biotopes with moderate and low temperatures (Prangishvili *et al.*, 2006).

---

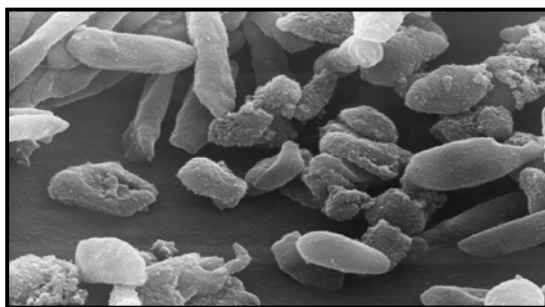
## 1.4. Virus $\phi$ Ch1 and its host *Natrialba magadii*

### 1.4.1. *Nab. magadii*

*Natrialba magadii* is the only known host for the temperate virus  $\phi$ Ch1. It is a haloalkaliphilic archaeon from the family of the *Halobacteriaceae*. *Nab. magadii* was first isolated from the soda lake Magadi in Kenya. It requires temperatures between 37°C and 42°C and an alkaline pH between 9 and 10 (Tindall *et al.*, 1980 and 1984). It also requires a salt concentration between 2 and 4 M NaCl to prevent cell lysis and a magnesium concentration less than 10 mM for optimal growth (Kamekura *et al.*, 1997).

*Nab. magadii* cells have a rod-shaped morphology, are orange-red, 0.2 to 0.7  $\mu$ m long, motile and grow strictly aerobically. Two different strains of *Nab. magadii* are available (Figure 2): The lysogenic strain L11 and the cured strain L13. Strain L11 carries the  $\phi$ Ch1 prophage and therefore shows features of temperate virus infection. Lytic growth of the phage durates until the stationary phase is entered. Then cell lysis and release of progeny phages appear (Figure 3). Lysogeny results in a stable co-existence with the host and is often achieved by integration into the host chromosome with the help of site-specific recombinases. Strain L13 is cured from  $\phi$ Ch1 through repetitive sub-culturing. This allows the usage of L13 as an indicator strain for infection with  $\phi$ Ch1.

L11



L13

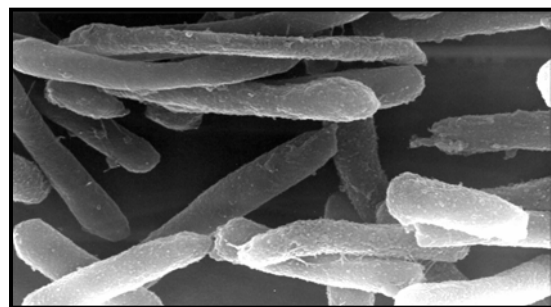


Figure 2: Electron micrograph of the wild type *Nab. magadii* L11, which carries  $\phi$ Ch1 as its prophage (left picture) and the indicator strain of *Nab. magadii*, L13 (right picture).

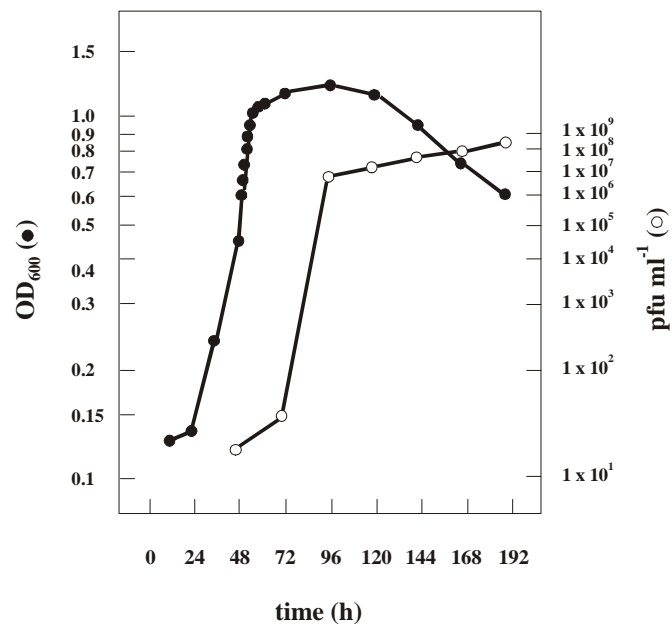


Figure 3: Growth and lysis curve of *Nab. magadii* L11 (●). After the cells reach the stationary phase lysis starts. (○) Indicates the release of viruses into the medium.

### 1.4.1. General aspects of $\phi$ Ch1

#### *Morphology of the virus $\phi$ Ch1*

Virus  $\phi$ Ch1 was the first virus isolated from an extreme haloalkaliphilic archaeon. The head-tail morphology resembles members of the family *Myoviridae* (Figure 4). The phage has an approximate size of 200 nm with 70 nm long heads and 130 nm long tails. The phage tail consists of an internal shaft which is covered by the contractile tail. The width of the tail is approximately 20 nm. The virus  $\phi$ Ch1 requires salt concentrations above 2 M NaCl (12%) otherwise a rapid decrease in infectivity can be observed. This can be due to dissociation of phage particles or significant conformational changes of the capsid proteins (Witte *et al.*, 1997).



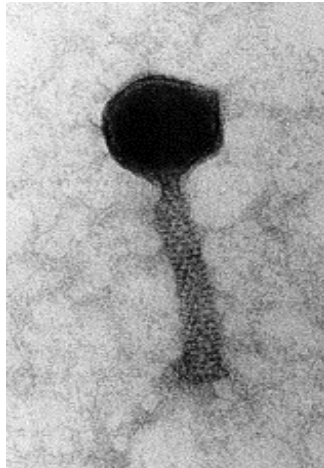


**Figure 4: Electron micrograph of a  $\phi$ Ch1 particle negatively stained with uranyl acetate. The head shows an icosahedral structure and the contractile tail covers the shaft.**

#### *Genome organization of $\phi$ Ch1*

The genome of  $\phi$ Ch1 consists of 58,498 bp linear double-stranded DNA and has an overall G+C content of 61.9%, which is typical for *Natronobacteria* (Tindall *et al.*, 1984).

The genome is terminally redundant and circularly permuted. These features suggest a headful packaging mechanism. The genome contains 98 open reading frames (ORF) and all of them have ATG as a start codon except of four ORFs that start with GTG. Many of the ORFs are overlapping and are therefore building transcriptional units (Klein *et al.*, 2002).

The  $\phi$ Ch1 DNA is partially methylated. One part of the genome is methylated at Dam-like sites whereas the other part is not methylated at these sites. No hemimethylated DNA strands were found. Although the *Nab. magadii* genome is not methylated, the following advantages seem possible: stability against nucleases, enzymatic selectivity in phage replication and transcription processes and protection against host-controlled restriction (Witte *et al.*, 1997).

All tailed dsDNA bacteriophages share a common genomic architecture i.e. organization of the genome into functional genetic modules (Figure 5). The

exchange of these modules between different virus populations may be a main mechanism of viral evolution (Hendrix *et al.*, 2000).

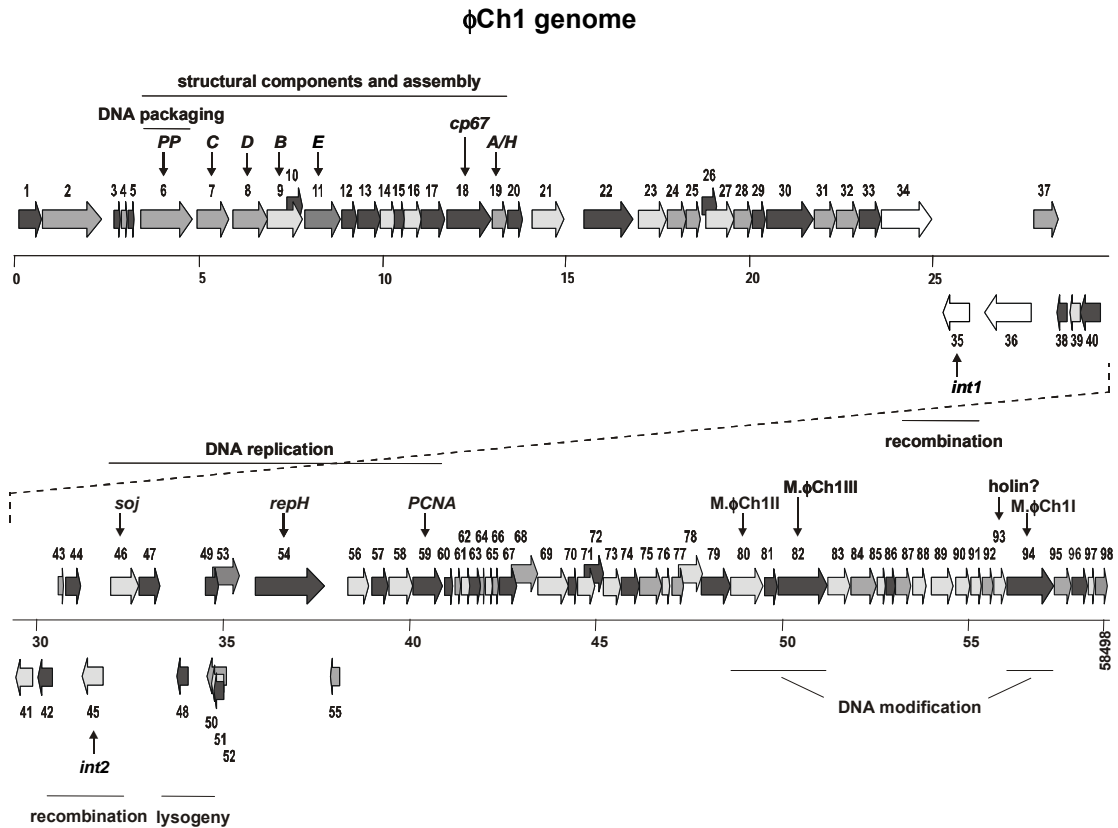


**Figure 5: Linear representation of the 58498 bp virus φCh1 genome starting at the *pac* site. ORFs are represented by arrows and numbered. Putative and verified functions of predicted gene products are indicated. The colors of the arrows indicate the frames of the ORFs: dark gray = 3<sup>rd</sup> reading frame, middle gray = 2<sup>nd</sup> reading frame and dark gray = 1<sup>st</sup> reading frame for both orientations.**

The φCh1 genome is organized into three parts. The left part contains clusters of genes coding for structural proteins and genes involved in virion morphogenesis. The right part of the genome contains genes for DNA methylation and restriction and several genes with unknown function. The genes in the left and right part are all transcribed rightwardly. The central part contains genes for replication, plasmid

---

stabilization and regulation of gene expression. Genes in this region are a mixture of rightwardly and leftwardly transcribed open reading frames (Klein *et al.*, 2002).  $\phi$ Ch1 is one of the four head-tail viruses with revealed DNA sequence. Only the genome sequences of the viruses'  $\phi$ M2,  $\phi$ M100 and HF2 are known (Pfister *et al.*, 1998; Luo *et al.*, 2001; Tang *et al.*, 2002). Although virus  $\phi$ H was studied very extensively no complete DNA sequence is available.  $\phi$ Ch1 and  $\phi$ H are very similar.  $\phi$ H infects the host *Halobacterium salinarum*. It resembles  $\phi$ Ch1 in several features.  $\phi$ H is a head-tail virus belonging to the family of *Myoviridae*. It has a linear double-stranded DNA, 59 kb in size. The ends are terminally redundant and the phage possesses a headful-packaging mechanism (Schnabel *et al.*, 1982a and 1982b). A characteristic of  $\phi$ H is the formation of a 12 kb large plasmid by recombination. This so-called L-plasmid contains besides the origin of replication, genes for immunity and early functions in the lytic phase (Schnabel *et al.*, 1984). The central part of the  $\phi$ Ch1 genome has sequence similarities of 50 to 97% to the L-plasmid of  $\phi$ H (Klein *et al.*, 2002). Although the hosts of these viruses are geographically very distant it is possible through pH gradients that halophilic and haloalkaliphilic species share the same environment (Hendrix *et al.*, 2000).

#### **1.4.2. Origin of replication of $\phi$ Ch1**

The development of a transformation system is fundamental for detailed investigation of the haloalkaliphilic archaeon *Nab. magadii* and its virus  $\phi$ Ch1. Transfection of *Halobacterium salinarum* with naked DNA was first developed by Cline and Doolittle (1987) and later on a PEG-mediated transformation method for *Haloferax volcanii* was established (Charlebois *et al.*, 1987). Shuttle vector systems for halophilic *Archaea* such as *Haloferax volcanii* and *Halobacterium salinarum* have already been described (Jolley *et al.*, 1996; Holmes and Dyall-Smith, 2000).

---

The origin of replication of  $\phi$ Ch1 is a good candidate for the development of a shuttle vector, which is recognized by *Nab. magadii* and therefore able to replicate in the host.

ORF54 starts with the codon GTG and encodes an 581 aa protein with a size of 65.2 kDa and a putative coiled-coil domain in the central part of the protein (Klein *et al.*, 2002). ORF54 shares similarities with the archaeal proteins encoded by *Hbt. salinarum* plasmid pHH1, *Hbt. salinarum* p $\phi$ HL, *Halobacterium sp.* (strain NRC-1) pNRC100 and *Hfx. volcanii* plasmid pHV2 (Klein *et al.*, 2002). Some of these proteins were shown to be essential for replication (Ng and DasSarma, 1993).

ORF54 ( $3 \times 10^{-45}$ ) and ORF53 ( $3 \times 10^{-7}$ ) of the  $\phi$ Ch1 DNA show similarities to the pNRC100 replication protein of *Haloarcula marismortui* (Baliga *et al.*, 2004). The C-terminal part of pNRC100 showed similarities to ORF54 and the N-terminal part to ORF53. Therefore it seems that the replication origin of  $\phi$ Ch1 contains two different open reading frames. However putative AT-rich promoter sequences could only be found at the 5' and 3' ends of the region containing ORF53 and ORF54. Therefore it is very likely that ORF53 and ORF54 are co-transcribed and co-translated. Inverted repeats were found downstream of ORF54 and upstream of ORF53, partially within the ORF49 and ORF55. These repeats could be involved in binding of replication proteins such as RepH, with the formation of a melted replication complex being facilitated by the AT-rich region (Kornberg and Baker, 1992; Schnos *et al.*, 1988). ORF49 as well as ORF55 seem to be involved in gene regulation.

### **1.4.3. Some aspects about gene regulation in $\phi$ Ch1**

The genome of  $\phi$ Ch1 contains at least one putative repressor gene with sequence similarities to the  $\phi$ H repressor (Klein *et al.*, 2002).  $\phi$ Ch1 ORF48 contains a winged helix-turn-helix DNA binding motif and a putative RecA self-cleavage site (Iro *et al.*, 2006). These two features are common for transcriptional repressors such as the LexA repressor and the biotin repressor in *E. coli* (Wilson *et al.*, 1992).

---

ORF48 is transcribed constitutively throughout the whole life cycle of  $\phi$ Ch1 (L11). Another putative repressor in this region is ORF49. Expression of ORF49 starts in the logarithmic and/or stationary phase. A doubling of the upstream part of ORF49 and the 5' part of ORF49 itself occurs in some virus populations. This mutation leads to a changed lysis behaviour (Iro *et al.*, 2006).

The intergenic region between ORF49 and ORF48 contains typical A-T rich promoter consensus sequences for halophilic *Archaea* (Soppa *et al.*, 1999). The repressor ORF48 shuts down the expression of ORF49 and therefore the promoter in the intergenic region of ORF48/ORF49. ORF49 seems to be connected to the lytic cycle as the similar transcript T4 of  $\phi$ H, which leads to activation of the lytic cycle (Stolt and Zillig, 1994). The expression of ORF49 is delayed in the lysogenic strain L11 compared to the expression of ORF48, but steadily increases during the virus life cycle until lysis. As ORF48 is constitutively expressed throughout the whole life cycle of  $\phi$ Ch1 there has to be a mechanism to stop its effect on repressing ORF49 to enter the lytic cycle. Possibly RecA mediated self-cleavage may be part of this system to induce ORF49 expression.

Gp43 and gp44 can partially relieve ORF48 mediated repression through interaction with the ORF48 coding sequence. The direct repeat at the 5' part of the sequence seems to be important for this interaction. The protein translated of ORF48 is not necessary for this effect (Iro *et al.*, 2006).

### **1.5. Site-specific recombination**

In site-specific recombination a recombinase interacts with corresponding binding sites in the DNA known as recombination core sites, brings the sites together in a synapse and then catalyzes strand exchange so that the DNA is cleaved and religated to opposite partners (Hallet and Sherratt, 1997). If two recombination sites point in opposite directions (inverted orientation), recombination results in

---

DNA inversion between the sites, but if they point in the same direction, recombination results in DNA excision (Sadowski, 1986).

The  $\lambda$  integrase family of site-specific recombinases consists of resolvases, transposases, excisionases/integrases and invertases. They can perform a variety of functions like integrative or excisive recombination of viral and plasmid DNA into and out of the host chromosome, conjugative transposition, resolution of catenated DNA circles, regulation of plasmid copy number, DNA excision to control gene expression or DNA inversions controlling the expression of cell surface proteins or DNA replication.

Recombinases of the  $\lambda$ -integrase family have a few features in common. They share conserved amino acid residues (R-H-R-Y, arg-his-arg-tyr) within the C-terminal half of the protein. The tyrosine within this conserved region is directly involved in the recombination reaction. Recombination occurs by formation and resolution of a holliday junction intermediate during which the recombinase is covalently linked to the DNA through the tyrosine residue (Nunes-Düby *et al.*, 1998; Groth and Calos, 2004; Guo *et al.*, 1997).

Site-specific recombination is often used to switch the expression of genes between different patterns. Genes controlled by this system often encode surface structure proteins *e.g.* bacteriophage tail fibres, flagellar antigens or pilins. The so reached genetic variability may help the virus to adapt to environmental changes. A good example is the so-called phase variation of *Salmonella enterica* serovar *Typhimurium*, where the inversion of a promoter sequence leads to the expression of different flagellar proteins (Zieg *et al.*, 1977).

The infection mechanism of tailed bacteriophages is often initiated by the interaction of a specific phage encoded protein with a receptor on the host cell wall. The variation of anti-receptor proteins by site-specific recombination can lead to a switch in the host range as shown for phage Mu and P1 (Plasterk *et al.*, 1983; Hiestand-Nauer and Iida, 1983).

The  $\phi$ Ch1 genome contains two open reading frames coding for putative site-specific recombinases of the  $\lambda$  integrase family (Klein *et al.*, 2002). Previously it

was suggested that the  $\phi$ Ch1 genome might integrate into the host chromosome (Witte *et al.*, 1997). So maybe these two ORFs are involved in integration. Possible other functions are decatenation of multimeric  $\phi$ Ch1 plasmids by reciprocal recombination between the virus palindromic (pal) sites to facilitate effective segregation of plasmid monomers into daughter cells during cell division or regulation of gene expression and plasmid copy number by inversion of DNA segments within the  $\phi$ Ch1 genome (Klein *et al.*, 2002).

In the central part of the  $\phi$ Ch1 genome lies ORF35 encoding for the putative site-specific recombinase Int1. Int1 shows highest similarities to other integrase proteins found in thermophilic *Archaea* and halophilic *Bacteria* such as *Mesorhizobium loti*, *Thermotoga maritima*, *Thermoplasma volcanium* and *Bacillus halodurans*. The flanking sequences of *int1* have several direct repeats, 30bps in length oriented in an inverted direction. These repeats are organized in clusters, IR-R and IR-L, and embedded in ORF34 and ORF36. The number of repeats varies among different virus particles (Table 1).

**Table 1. Number of repeats within proteins encoded by ORF34 and ORF36 and derivatives (Rössler *et al.*, 2004).**

Clone	ORF34			ORF36			Orientation
	No. of repeats	pl	MW (kDa)	No. of repeats	pl	MW (kDa)	
pBgB1	14	3.67	47.94	6	3.69	44.95	+
pBgB5	13	3.7	52.99	8	3.65	39.89	+
pBgB43	4	3.82	51.09	14	3.63	41.26	-
pBgB51	13	3.69	54.00	7	3.66	38.89	+
pBgB52	9	3.69	54.66	14	3.63	41.26	-

ORF34 and ORF36 share an amino acid identity of 33% due to the repeats. Where 5'-ATGGAcgC-3' is the most conserved sequence found. Therefore it is not surprising that, both proteins were recognized by an  $\alpha$ ORF36 antiserum. They are

---

also recognized by an  $\alpha\phi$ Ch1 antiserum leading to the suggestion that both proteins are part of the mature virus particle.

Inversion within this region leads to an exchange of the C-terminal regions of ORF34 and ORF36 (Figure 6). A possible mechanism that results in this exchange is described in the following: (i) intramolecular recombination between direct repeats, that can lead to the formation of circular intermediates, (ii) intermolecular crossing over event that did not occur exactly between two corresponding repeats and leads to different numbers of repeats compared to the parental DNA, (iii) intermolecular recombination between ORF34 and ORF36, (iv) intermolecular recombination between to different ORF34 genes.

Only the ORF34 but not the ORF36 upstream region carries a functional promoter therefore it is not surprising that only ORF34 but not ORF36 is expressed in the lysogenic strain *Nab. magadii* L11. Transcription of ORF34 starts at the transition from the logarithmic to the stationary growth phase of the host strain (Figure 7 A and B).

Gp34<sub>52</sub> contains the 3' part of ORF36 and binds to the cell surface of *Nab. magadii* L13. The C-terminal part of gp34<sub>52</sub> contains a galactose binding domain, which binds to specific cell surface attached galactose molecules (Rössler *et al.*, in prep.). Galactose can often be found as part of carbohydrate residues in archaeal S-layer proteins (Mengele and Sumper, 1992). In the presence of  $\alpha$ -D-galactose an inhibition of phage infection can be observed, therefore it seemed obvious that the binding of the phage to the host cell depends on these glycosylated structures. These results were confirmed by binding assays with gp34<sub>1</sub> and the C-terminal part of gp34<sub>52</sub> alone. Gp34<sub>1</sub> was not able to bind to the S-layer whereas the C-terminus of gp34<sub>52</sub> was.

Int1 is constitutively expressed during the life cycle of *Nab. magadii* L11 whereas the expression increased clearly after the third day after inoculation in the mid-logarithmic growth phase. Corresponding to this the inversion reaction is detectable through PCR at day 3 and 4 after inoculation (Rössler *et al.*, in prep.).



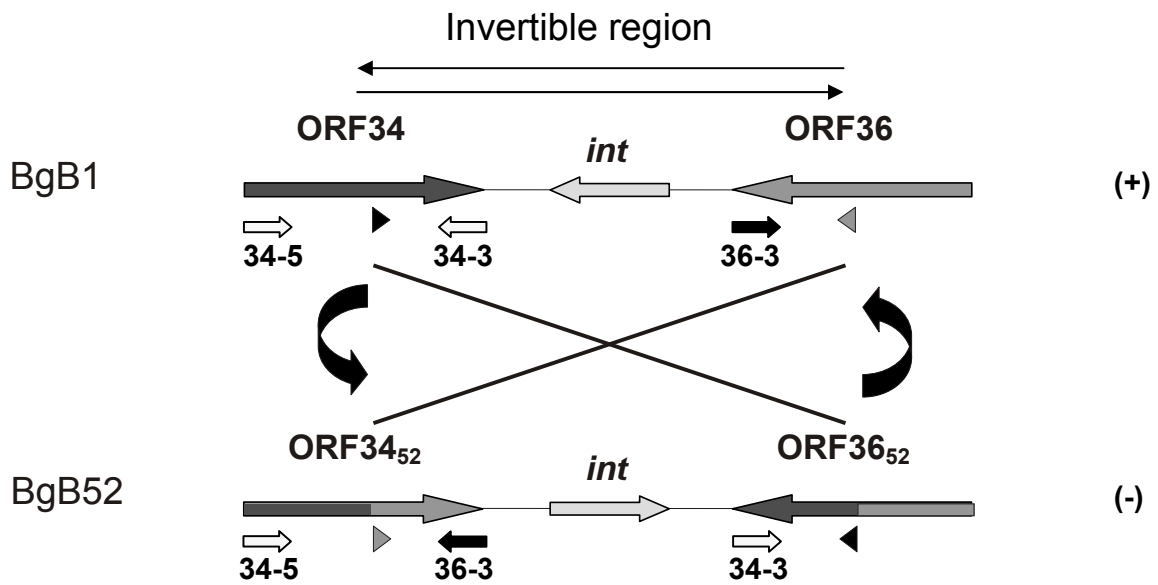


Figure 6: The invertible region of  $\phi$ Ch1: Inversion exchanges the 3' ends of the open reading frames 34 and 36. The open reading frames of the integrase as well as the flanking open reading frames are indicated by arrows.

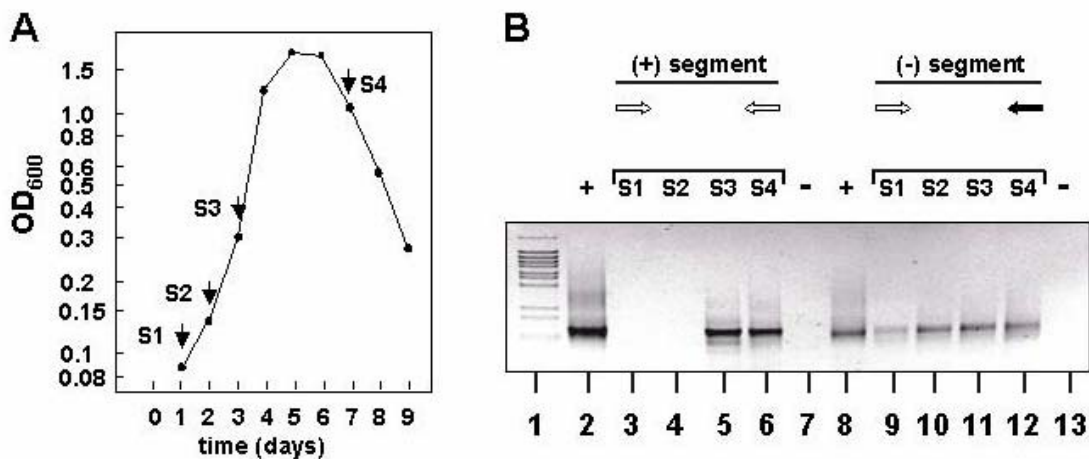


Figure 7: The invertible region of  $\phi$ Ch1. **A:** Growth and lysis of a lysogenic strain of *Nab. magadii*. Vertical asterisks indicate the time points of sample collection **B:** Time kinetics of the inversion reaction. Cell extracts were taken at different time points and used for PCR analysis to amplify ORF34. Primers used were (i) 34-5 and 34-3, in order to amplify ORF34 of the (+) segment (lanes 2 – 7) or (ii) 34-5 and 36-3, in order to amplify ORF34 of the (-) segment with the exchanged C-terminus (lanes 8 - 13).



---

## 2. Materials and methods

### 2.1. Methods

#### 2.1.1. Archaeal strains

---

Strain	feature	reference
<i>Nab. magadii</i> L11	wt, $\phi$ Ch1 provirus	Witte <i>et al.</i> , 1997
<i>Nab. magadii</i> L13	cured of $\phi$ Ch1	Witte <i>et al.</i> , 1997
<i>Hfx. volcanii</i> WFD11	cured of plasmid pHV2	Charlebois <i>et al.</i> , 1987
<i>Hbt. salinarum</i> R1		Schnabel <i>et al.</i> , 1982a
<i>Hrr. coriense</i>	wt	DSM 10284
<i>Hrr. lacusprofundi</i>	wt	DSM 5037
<i>Hrr. saccharovorum</i>	wt	Tomlinson and Hochstein, 1976
<i>Hrr. sodomense</i>	wt	DSM 3755
<i>Nbt. gregoryi</i>	wt	DSM 3393
<i>Nmn. pharaonis</i>	wt	DSM 2160
<i>Nab. asiatica</i>	wt	DSM 12278

---

## 2.1.2. Bacterial strains

---

Strain	feature	reference
XL1-Blue	<i>endA1, gyrA96, hsdR17 (r<sub>k</sub><sup>-</sup>m<sub>k</sub><sup>+</sup>), lac, recA1, relA1, supE44, thi, (F', lac<sup>f</sup>, lacZΔM15, proAB<sup>+</sup>, tet)</i>	Stratagene
JM110	<i>F', traD36, lac<sup>f</sup>Δ(lacZ)M15, proA<sup>+</sup>B<sup>+</sup>/rpsL, thr, leu, thi, lacY, galK, galT, ara, fhuA, dam, dcm, glnV44, Δ(lac-proAB)</i>	Yanisch-Perron <i>et al.</i> , 1985

## 2.1.3. Plasmids

---

Plasmid	feature	reference
pMDS11 1991	<i>bla, ColE1, pHK2 origin, gyrB (Nov<sup>R</sup>)</i>	Holmes <i>et al.</i> , 1991
pMDS24	<i>bla, ColE1, Mev<sup>R</sup>, DHFR, pHV2 ori</i>	Jolley <i>et al.</i> , 1996
pKS <sub>II</sub> <sup>+</sup>	<i>mcs, bla, ColE1, lacZα</i>	Stratagene
pBAD24	<i>mcs3, pBRori, araC, bla</i>	Guzman <i>et al.</i> , 1995
pUC19	<i>bla, pMB1ori, lacZα, mcs</i>	Yanisch-Perron <i>et al.</i> , 1985

---

pBgB52	BgIII-fragment B52 of $\phi$ Ch1 cloned into pKS <sub>II</sub> <sup>+</sup>	Rössler <i>et al.</i> , 2004
pBgB52 $\Delta$ int1	pBgB52, $\Delta$ int1	R. Dobetsberger
pBgB1	BgIII-fragment B1 of Ch1 cloned into pKS <sub>II</sub> <sup>+</sup>	Rössler <i>et al.</i> , 2004
pNov-1	<i>gyrB</i> (Nov <sup>R</sup> ) fragment (SmaI-HindIII fragment from pMDS11) introduced into pKS <sub>II</sub> <sup>+</sup> at position nu. 330	Iro <i>et al.</i> , in prep
pRo-1	nu. 34656-37593 of $\phi$ Ch1 introduced into pNov-1	this study
pRo-2	nu. 34656-37978 of $\phi$ Ch1 introduced into pNov-1	this study
pRo-3	nu. 33951-34479/34626-37978 of $\phi$ Ch1 introduced into pNov-1	this study
pRo-4	nu. 33951-37978 of $\phi$ Ch1 introduced into pNov-1	this study
pRo-5	nu. 33951-34479/34626-37765 of $\phi$ Ch1 introduced into pNov-1	this study
pRo-6	nu. 33951-37978 of $\phi$ Ch1 introduced into pNov-1	this study
pUC 52-1	ORF34 of pBgB52 introduced into pUC19	this study
pUC 52-2	ORF36 and ORF35 ( <i>int1</i> ) of pBgB52 introduced into pUC 52-1	this study
pUC 52-3	ORF36 of pBgB52 $\Delta$ int1 introduced into pUC 52-2	this study

---

pRo-5 52-2	ORF34, ORF35 and ORF36 of pUC 52-2 introduced into pRo-5	this study
pRo-5 52-3	ORF34 and ORF36 of pUC 52-3 introduced into pRo-5	this study
pBAD24-int1	ORF35 introduced into pBAD24	this study
pIR-28-int1	Spacer sequence with two single indirect repeats introduced into pBAD-int1	this study
pDR-28-int1	Spacer sequence with two single direct repeats introduced into pBAD-int1	this study
pIRM1-28-int1	pIR-28-int1 with a point mutation in the 5' repeat sequence	this study
pIRM4-28-int1	pIR-28-int1 with a point mutation in the 5' repeat sequence	this study
pIRM7-28-int1	pIR-28-int1 with a point mutation in the 5' repeat sequence	this study
pIRM11-28-int1	pIR-28-int1 with a point mutation in the 5' repeat sequence	this study
pIR <sub>17</sub> -28	Spacer sequence with two multiple repeat clusters including an overlapping inverted repeat introduced into pBAD-int1	this study
pIR <sub>16</sub> -28	Spacer sequence with two multiple repeat clusters introduced into pBAD-int1	this study

---

#### 2.1.4. DNA marker

GeneRuler 1kb DNA ladder plus (Fermentas):

20000, 10000, 7000, 5000, 4000, 3000, 2000, 1500, 1000,  
700, 500, 400, 300, 200, 75 bp

$\lambda$ /BstEII: 8453, 7242, 6369, 5687, 4822, 4324, 3675, 2323, 1929, 1371,  
1264, 702, 224, 117 bp

pUC19/HaeIII: 587, 488, 434, 309, 267, 257, 174, 102, 80, 18, 11 bp

#### 2.1.5. Protein marker

Unstained Protein Molecular Weight Marker #SM0431 (Fermentas):

MW: 116; 66,2; 35; 25; 18.4; 14.4 kDa

#### 2.1.6. Primer

---

Primer	sequence
--------	----------

---

Ro1	5'- CAGAT <u>GGTACCGG</u> AGTGGTTGGACACTC -3'
Ro2	5'- CATGGA <u>AAGCTT</u> CAGTCAGCCCCGG -3'
Ro3	5'- CATGGA <u>AAGCTT</u> ACTGTCATCGATGGTTTG -3'
Ro5	5'- CAGGT <u>CTAGACCG</u> GTTGAAGGCAGCTT -3'
Ro6	5'- AATT <u>CCCGGG</u> CTGGTATGGTG -3'

---

Ro7 5'- AATTCCCGGGGGCCGTG -3'  
 TR1 5'- AATTGCGGCCGCGCGTTGAAGGCA -3'  
 TR2 5'- AATTTCTAGATCCTGGGCCTCTTTGAA -3'  
 TR3 5'- AATTTCTAGAACGCTCACGAAAAATCA -3'  
 TR4 5'- GCAGAAAGCTTCGGCGTGATCGCGAGTAAAA -3'  
 pHV2-1 5'- GCCAAAGAGAAAGAGCGA -3'  
 pHV2-2 5'- AGTCGACAGAGTCAGCCAA -3'  
 JasInt5 5'-ACGTCCATGGCGCATCACCATCACCATCACATGTCCAAA  
 GAGAGACATGC -3'  
 Int13-Xba 5'- CAGCATCTAGAAAGGATGAAGTGGCGCG -3'  
 IR-L-Hind 5'- GACTAAAGCTTCATATGGACGCGGTGAGCGACTCCCAGAC  
 GGCACGCCGAGGAGGTTCT -3'  
 IR-R-Xba 5'- GCTATCTAGAGTAATGGACGCGGTAAGTACGTCCGAGAC  
 GGCCGCCATCGCAACGAAC -3'  
 DR-R-Xba 5'- GCTATCTAGAGTAGGCCGTCTCGGACGTACTTACCGCGT  
 CCATGCCATCGCAACGAAC -3'  
 IR-R-Xba $\Delta$  5'- GCTATCTAGAGTAATGGACGCGCCATCG -3'  
 IR-M1 5'- GCTATCTAGAGTAATAGACGCGGTAAGTA -3'  
 IR-M4 5'- GCTATCTAGAGTAATGAACGCGGTAAGTA -3'  
 IR-M7 5'- GCTATCTAGAGTAATGGTCGCGGTAAGTA -3'  
 IR-M11 5'- GCTATCTAGAGTAATGGAAGCGGTAAGTA -3'  
 CH3-8 5'- CTGAGAAGTACATCCGGATTT -3'  
 p28 plus 5'- TCTGGCCTGAATGACGA -3'  
 p28 minus 5'- GAGCCGTGTTCTGTTCTG -3'  
 pBAD-R 5'- CGGCGTTTCACTTCTGA -3'  
 A7 5'- CAGGCTGCAGTCGACCAGATCGTGTCG -3'  
 A8 5'- CAGGAAAGCTTGACATCGCGCTACCG -3'  
 28-Sma 5'- CAGGCCCGGGCGCCGAGGAGGTTCT -3'  
 28-Pst 5'- CAGGCTGCAGCCATCGCAACGAAC -3'  
 34-5 5'- CAGCAGAGATCTATGAGTAAAATCTGGGAACCGAG -3'  
 A4k 5'- CATGCCCGGGTCTTCGACAATCGTCCG -3'  
 A4 5'- CAGGCCCGGGTCAGAGTCGAAGAGCGC -3'



---

Int-Bam	5'- GACGCGGATCCGGCTAGCAGGAGGAATT -3'
Int-Sma	5'- CAGCACCCGGGAGGATGAAGTGGCGCG -3'
34-Kpn	5'- CAGCAGGGTACCCGGCGTTCGAGGTCA -3'
34-3-Xba	5'- CAGCTCTAGAGTATATCCCTCGTCGAAG -3'
36-51-Xba	5'- CAGCTCTAGAGCCAGATAGGTCACCAGTGT -3'
36-5-Hind	5'- GACGACAAGCTTATGGATCCGATCAGCG -3'
36-3	5'- CAGCAGAAGCTTATTCAGGTTTCATGTCGCTG -3'
34-3	5'- CAGCAGAAGCTTCAGATCAGGTTTATATTGCTGAAGT -3'

Underlined sequences mark recognition sites for restriction endonucleases.

### 2.1.7. Restriction enzymes and buffers

Restriction endonucleases and their corresponding buffers were obtained by Fermentas and New England BioLabs. Buffer concentrations were used as suggested.

### 2.1.8. Media

#### LB-Medium

Peptone	10 g
Yeast extract	5 g
NaCl	5 g

pH 7.5

Add distilled water to give a final volume of 1l

15g/l Agar were added for plates

#### NVM (Natrialba rich medium)

---

Casein hydrolysate	8.8 g
Yeast extract	11.7 g
Na <sub>3</sub> -Citrate	0.8 g
KCl	2.35 g
NaCl	235 g

pH 9

dH<sub>2</sub>O was added to a final volume of 935 ml before autoclaving.

After autoclaving the medium was completed with:

0.57 M Na <sub>2</sub> CO <sub>3</sub>	65 ml
1 M MgSO <sub>4</sub>	1 ml
1 M FeSO <sub>4</sub> ·7H <sub>2</sub> O	1 ml

8g/l Agar were added for plates

DSMZ Medium 372: Halobacteria medium

Yeast extract	5g
Casamino acids	5g
Na-glutamate	1g
KCl	2g
Na <sub>3</sub> -citrate	3g
MgSO <sub>4</sub> x 7 H <sub>2</sub> O	20g
NaCl	200g
FeCl <sub>2</sub> x 4 H <sub>2</sub> O	36mg
MnCl <sub>2</sub> x 4 H <sub>2</sub> O	0,36mg

Add distilled water to give a final volume of 1l

Adjust pH to 7.0 - 7.2

10g/l Agar were added for plates

---

### 18% MGM (modified growth medium)

Salt water (30% stock)	600ml
dH <sub>2</sub> O	367ml
Peptone	5g
Yeast extract	1g

Adjust pH to 7.5 with Tris-HCl pH 9.5

Add distilled water to give a final volume of 1l

10g/l Agar were added for plates

### Salt water stock solution – 30% (w/v)

NaCl	240g
MgCl <sub>2</sub> x 6 H <sub>2</sub> O	30g
MgSO <sub>4</sub> x 7 H <sub>2</sub> O	35g
KCl	7g
CaCl <sub>2</sub> x 7 H <sub>2</sub> O	0,74g

Adjust pH to 7.5 with Tris-HCl pH 7.5

Add distilled water to give a final volume of 1l

## **2.1.9. Antibiotics – stock solutions**

Antibiotic	Stock	Final conc.	comment
Ampicillin	20mg/ml	100µg/ml	in ddH <sub>2</sub> O, sterile, 4°C
Tetracycline	10mg/ml	10µg/ml	in 70% EtOH, light protected, -20°C
Mevinolin	10mg/ml	4µg/ml	in 70% EtOH, -20°C
Novobiocin	3mg/ml	1,5-12µg/ml	in ddH <sub>2</sub> O, sterile, -20°C

---

### 2.1.10. Antibodies

#### Primary antibodies

Antibody dilution	comment	Final
$\alpha$ His-taq antibody	against His taq epitope, mouse	1:5000
$\alpha$ ORF36 antibody	against ORF36 of the phage $\Phi$ Ch1, rabbit	1:2500

Primary antibodies were diluted in 1xTBS, 0,3%BSA, 0,02%NaN<sub>3</sub>.

#### Secondary antibodies

Antibody dilution	comment	Final
$\alpha$ -rabbit Ig	linked to Horseradish Peroxidase	1:5000
$\alpha$ -mouse Ig	linked to Horseradish Peroxidase	1:5000

Secondary antibodies were diluted in 1xTBS.

### 2.1.11. General buffers and solutions

#### Solutions for *E. coli* methods

##### MOPS I

100mM MOPS  
10mM CaCl<sub>2</sub>  
10mM RbCl  
pH 7.0

##### MOPS II

100mM MOPS  
70mM CaCl<sub>2</sub>  
10mM RbCl  
pH 6.5

##### MOPS IIa

100mM MOPS  
70mM CaCl<sub>2</sub>  
10mM RbCl  
15% glycerol  
pH 6.5

---

## **Solutions for archaeal methods**

### **Buffered Spheroplasting solution**

Low Salt without glycerol

1M NaCl

27mM KCl

50mM TrisHCl pH 8.2

15% sucrose

### **Buffered Spheroplasting solution**

Low Salt with glycerol

1M NaCl

27mM KCl

50mM TrisHCl pH 8.2

15% sucrose

15% glycerol

### **Buffered Spheroplasting solution**

High Salt without glycerol

2M NaCl

27mM KCl

50mM TrisHCl pH 8.2

15% sucrose

### **Unbuffered Spheroplasting solution**

Low Salt

1M NaCl

27mM KCl

15% sucrose

### **Unbuffered Spheroplasting solution**

High Salt

2M NaCl

27mM KCl

15% sucrose

## **Solutions for Protein methods**

### **Coomassie staining solution**

25% MeOH

10% acetic acid

0,15% Coomassie Blue R250/G250

### **Coomassie destaining solution**

25% MeOH

10% acetic acid

---

**30% PAA**

29,2% acrylamide  
0.8% N,N'-methylene bisacrylamide

**10x SDS running buffer**

0.25M Tris base  
1.92M glycine  
1% SDS

**4x Resolving gel buffer**

1.5M TrisHCl pH 8.8  
0.4% SDS

**10x TBS**

8% NaCl  
3% Tris base  
0,2% KCl  
pH 8.0

**Ponceau S**

0,5% Ponceau S  
3% trichloroacetic acid

**2x protein sample buffer**

0.12mM TrisHCl pH 6.8  
4% SDS  
17,4% glycerol  
2%  $\beta$ -mercaptoethanol  
0.02% bromphenol blue

**4x Stacking gel buffer**

0.5M TrisHCl pH 6.8  
0.4% SDS

**Transblotbuffer**

48mM Tris base  
39mM glycine  
0.037% SDS (v/v)  
20% MeOH

**Solutions for DNA methods****6% PAA gel**

6% PAA in 1x TBE  
60  $\mu$ l 10%APS  
6  $\mu$ l TEMED

**50x TAE**

2M Tris base  
1M acetic acid  
0,1M EDTA  
pH 8.2

---

**10x TBE**

89mM Tris base  
89mM boric acid  
2mM EDTA  
pH 8.2

**λ Marker**

10 µl digested –DNA (*Bst*EII digested,  
500 µg/ml)  
70 µl ddH<sub>2</sub>O  
20 µl 5x DNA sample buffer  
10min 60°C – denaturing the DNA  
Store at -20°C

**Solution 2**

0,2N NaOH  
1% SDS

**Blocking solution**

7.3g NaCl  
2.41g Na<sub>2</sub>HPO<sub>4</sub>  
0.96g NaH<sub>2</sub>PO<sub>4</sub>  
49.89g SDS  
pH 7.2, add ddH<sub>2</sub>O to 1l

**5x DNA sample buffer**

25% sucrose  
0.05% bromphenol blue  
0.1% SDS  
50mM TrisHCl pH 8.2

**Solution 1**

50mM glucose  
25mM TrisHCl pH 8.0  
10mM EDTA pH 8.0  
10 µg/ml RNaseA  
Store at 4°C

**Solution 3**

3M KAc  
pH 4.8

**10x Washing solution II**

12.1g Tris base  
5.85g NaCl  
2.03g MgCl<sub>2</sub>  
pH 9.5, add ddH<sub>2</sub>O to 1l

---

**Hybridisation buffer**

55ml ddH<sub>2</sub>O

25ml 20x SSC

10ml 50x Denhardt's solution

5ml 10% BSA

5ml 1M NaH<sub>2</sub>PO<sub>4</sub>

500 µl 20% SDS

200 µl 0,5M EDTA

**20x SSC**

3M NaCl

0,3M sodium citrate

pH 7.2

**50x Denhardt's solution**

1g Ficoll 400

1g Polyvinylpyrrolidone

1g BSA

Add ddH<sub>2</sub>O to 100ml; store at -20°C



---

## **2.2. Methods**

### **2.2.1. *E. coli* methods**

#### **2.2.1.1. MOPS competent cells**

100ml LB-medium was inoculated with 2ml of an *E. coli* XL1B or JM110 overnight culture and grown to an OD<sub>600</sub> of 0.6 at 37°C. The cells were collected (5000rpm, 5min, 4°C) and resuspended in 40ml cold MOPS I solution. After incubation on ice for 10min the cells were centrifuged (5000rpm, 5min, 4°C) before they were resuspended in 40ml cold MOPS II solution. The solution was incubated for 30 min on ice and then centrifuged once more at 5000rpm for 5min at 4°C. The pellet was finally resuspended in 2ml MOPS IIa and incubated for 10min on ice. 100 µl aliquotes were used freshly or stored at -80°C.

#### **2.2.1.2. Transformation of MOPS competent cells**

To transform competent *E. coli* cells 1 µl of Plasmid DNA or 15 µl of ligated DNA were mixed with 100 µl fresh or frozen competent cells. After incubation for 30min on ice the cells were heat shocked for 2min at 42°C. Before adding 300 µl of LB media the cells were put on ice for a short period of time. Then the cells were put on 37°C for 30min to regenerate. 100 µl of regenerated cells were plated on every LB selective plate. The plates were incubated upside down over night at 37°C.

---

## **2.2.2. Archaeal methods**

### **2.2.2.1. Phage titers**

300  $\mu$ l *Nab. magadii* L13 cells and 100  $\mu$ l of  $\phi$ Ch1 phage dilutions ( $10^{-3}$  -  $10^{-9}$ ) were mixed with 5ml NVM soft agar and poured on NVM plates. The plates were incubated at 37°C for two weeks.

### **2.2.2.2. Transformation of halophilic and haloalkaliphilic archaea**

The culture was incubated with 70  $\mu$ g/ml bacitracin at 37°C to an OD<sub>600</sub> of 0.5-0.65. The culture was collected (6000rpm, 15min) and resuspended in buffered spheroplasting solution with 20 $\mu$ g/ml proteinase K for two days at 42°C by shaking. Aliquotes of 1.5 ml were pelleted and resuspended in 150  $\mu$ l buffered spheroplasting solution with 15  $\mu$ l 0,5M EDTA pH 8.0. The mixture was left 5min at room temperature until spheroplasts have formed. 1-10 $\mu$ g of DNA were added and incubated for 10min. An equal volume of 60% PEG<sub>600</sub> (diluted with unbuffered spheroplasting solution) was added, mixed well and incubated for 30min at room temperature. The cells were washed with 1ml media and regenerated in 1ml media over night at 37°C by shaking.

The next day 100  $\mu$ l were plated on every agar plate.

For the transformation of *Hfx. volcanii*, *Hrr. sodomense*, *Hrr. coriense*, *Hrr. lacusprofundi* and *Hrr. saccharovororum* low salt spheroplasting solutions were used and for *Nab. magadii*, *Nmn. pharaonis*, *Nbt. gregoryi* and *Hbt. salinarum* high salt spheroplasting solutions were used.

*Hfx. volcanii* and *Hbt. salinarum* cells weren't incubated with bacitracin and proteinase K but grown to an OD<sub>600</sub> of 0.6-0.9. The four *Halorubrum* strains were incubated with proteinase K but not with bacitracin.

---

### **2.2.2.3. Isolation of plasmid DNA from halo(alkali)philic *Archaea* and retransformation**

1-5  $\mu$ l of plasmid DNA prepared by a modified alkaline lysis procedure (<http://www.microbiol.unimelb.edu.au/people/dyallsmith/HaloHandbook/>) were transformed into MOPS competent *E.coli* XL1B cells. Confirmation of plasmids isolated from halo(alkali)philic *Archaea* was performed by PCR analysis using primers TR-1/TR-4 and CJ3-1/CJ3-2.

### **2.2.2.4. Plasmid copy number determination**

The number of plasmids per cell was determined by extracting plasmid DNA from cultures in mid-log phase, multiple times. Different amounts of plasmid DNA were run on an 0.8% agarose gel. The intensities of the ethidium bromide stained bands were compared to DNA marker bands with known concentrations. Through plating serial dilutions on agar plates the number of viable cells used for plasmid preparations were determined. The plates were incubated at 37°C for four weeks.

## **2.2.3. DNA methods**

### **2.2.3.1. Polymerase chain reaction**

For DNA amplification reactions *Pwo* DNA-Polymerase (peQLab) was used.

Batch:           1  $\mu$ l template DNA  
                  10  $\mu$ l 10x PCR reaction buffer  
                  10  $\mu$ l 2mM dNTPs  
                  500 ng 3' primer (5  $\mu$ l)

---

500 ng 5' primer (5  $\mu$ l)  
2  $\mu$ l *Pwo* DNA-Polymerase (2U)

ddH<sub>2</sub>O was added to a final volume of 100  $\mu$ l. The batch was overlaid with paraffin.

PCR program:

Step1:	denaturation	94°C	4min
Step2:	denaturation	94°C	1min
Step3:	annealing	X	1min
Step4:	elongation	72°C	1min/1000bp fragment
Step5:	elongation	72°C	dependant on DNA fragment length
Step6:		4°C	$\infty$

The annealing temperature was set 4°C lower than the melting temperature of the primers.

From step 2 to step 4 33 cycles were performed.

### **2.2.3.2. Purification of PCR and DNA fragments**

Purification of DNA fragments was performed by the QIAquick PCR purification kit from QIAGEN. If fragments were eluted from agarose gels the QIAquick Gel extraction kit was used.

### **2.2.3.3. Restriction of DNA**

For restriction amounts of DNA and restriction enzymes were used as suggested from the manufacturer.

---

#### **2.2.3.4. Ligation of DNA**

T4 DNA Ligase and the corresponding 10x T4 Ligase buffer were provided from Fermentas. Vector and fragment were set in a ratio of 1:4. The ligation batch was incubated three hours at room temperature or over night at 16°C.

#### **2.2.3.5. Plasmid preparation**

##### Quick preparation method

For a fast screening of clones the quick preparation method was used.

300 µl of an overnight culture were collected by centrifugation and resuspended in 30 µl of 5x DNA sample buffer. 14 µl phenol/chloroform (1:1) were added and mixed well by vortexing. After centrifugation for 5min at 13.2krpm 12 µl of the supernatant was applied to a 0.8% agarose gel.

##### Alkaline lysis method

3ml of an overnight culture were collected by centrifugation and resuspended in 100 µl lysisbuffer (solution 1). After addition of 200 µl SDS/OH (solution 2) the batch was gently mixed until the mixture becomes clear. Then 150 µl 3M KAc (solution 3) were added, the batch was mixed and centrifuged for 15min at 4°C. The supernatant was transferred to a fresh tube and phenol/chloroform extraction followed.

##### Phenol/Chloroform extraction

The resulting supernatant from alkaline lysis is mixed with 200 µl phenol and 200 µl chloroform. After centrifugation (2min, 13krpm, 4°C) the aqueous phase was transferred to a fresh tube and 200 µl of chloroform were added to remove phenol

---

residues. The batch was again centrifuged and the supernatant was transferred to a fresh tube ready for precipitation.

#### DNA precipitation

2.5 volumes of 96% ethanol were added to the phenol/chloroform extracted supernatant. The tube was incubated 30min at -20°C or 15min at -80°C. Afterwards it was centrifuged for 35min with 16,4krpm at 4°C. The resulting pellet was washed two times with 70% EtOH to remove protein residues and dried at 65°C until the ethanol was vaporized. The pellet was resuspended in 30-50 µl ddH<sub>2</sub>O.

#### Plasmid mini preparation

Mini preparations of plasmid DNA were performed by the peqGOLD Plasmid Miniprep Kit from peqLab.

### **2.2.3.6. Agarose gel electrophoresis**

The separation of DNA-fragments in an electric field was performed using 0.8% or 1.5% (w/v) agarose gels. 1xTAE was used as a buffer and an impressed voltage of 100V was used.

### **2.2.3.7. Southern blot**

Southern blot is a method to visualize specific DNA fragments separated on an agarose gel.

---

To denature the DNA the agarose gel was incubated in 0.4N NaOH/ 0.6M NaCl for 30min. Neutralization of DNA took place in 1.5M NaCl / 0.5M Tris-HCl pH 7.5 for 30min.

A nitrocellulose membrane cut into the dimension of the agarose gel was equilibrated in 10x SSC. The transfer was performed by a capillary blot with 10x SSC as transfer solution over night.

After transfer the membrane was laid into 0.4N NaOH for one minute and afterwards in 0.2M Tris-HCl pH 7.5 again for one minute. After drying of the membrane it was fixed through UV-crosslinking.

#### Labelling reaction

For hybridisation the probe was labelled with biotin. Therefore x µl DNA were diluted up to 34 µl with ddH<sub>2</sub>O and boiled for 10min to denature the DNA. The labelling reaction was mixed as follows: 34 µl DNA

10 µl 5x Labelling Mix

5 µl dNTP Mix

1 µl Klenow fragment

The mixture was incubated on 37°C for 3 hours.

The reaction was stopped by adding 0.5 µl 0,2M EDTA pH 8.0. Precipitation of the DNA was reached with the addition of 5 µl 4M LiCl and 150 µl 96% EtOH. After incubation for 20min at -20°C the batch was centrifuged (13krpm, 30min, 4°C). The pellet was washed with 70% EtOH and after drying resuspended in 20 µl ddH<sub>2</sub>O.

#### Prehybridisation and hybridisation

Before the actual hybridisation with the labelled probe can take place the membrane has to be prehybridised for three hours at 65°C to block unspecific binding sites.

Per hybridisation flask 12ml hybridisation buffer were mixed with 120 µl salmon sperm DNA (10mg/ml).

After prehybridisation the labelled probe was denatured for 5min at 95°C, shortly put on ice and added to the hybridisation flasks. Hybridisation was performed over

---

night at 65°C. Then the membrane was washed two times with 2x SSC / 0.1% SDS for 5min at room temperature and two times with 0.1x SSC / 0.1% SDS for 15min at 65°C.

#### Development of the blot

The following steps were performed at room temperature.

The membrane was washed 5min with blocking solution. Then it was incubated for 5min with streptavidin solution: 7ml blocking solution + 7 µl streptavidin. Afterwards the membrane was washed three times for 5min with a 1:10 dilution of the blocking solution, followed by 5min incubation with biotinylated alkaline phosphatase solution: 7ml blocking solution + 7 µl biotinylated alkaline phosphatase. The blot was again washed for 5min with blocking solution followed by three additional washing steps with washing solution II. Then the blot was incubated for 5min with CDP-Star reagent: 3ml dilution buffer + 6µl CDP-Star and finally developed in the dark room.

### **2.2.4. Protein methods**

#### **2.2.4.1. Overexpression of proteins in *E. coli***

A freshly inoculated culture was incubated at 37°C until an optical density of 0.3 was reached. Induction of expression was performed through the addition of 0.2% arabinose. Before induction and different time points after induction protein samples were taken. Therefore, 1.5 ml culture was collected. The pellet was then resuspended in  $x$  µl of 5mM Na-phosphate buffer ( $x = OD_{600} \times 75$ ) and the same volume of 2x protein sample buffer was added. After boiling of the samples for 10min the samples were analysed on a SDS-PAGE.



---

#### 2.2.4.2. Expression of proteins in *Nab. magadii*

A freshly inoculated culture was incubated at 37°C. Protein samples were taken several times a day starting at an OD<sub>600</sub> of 0.1 as described for *E. coli* protein samples.

For PCR templates 1.5ml culture was collected and resuspended in x µl of ddH<sub>2</sub>O.

#### 2.2.4.3. SDS PAGE (Laemmli system)

For protein analysis the BIORAD Miniprotean vertical gel system was used.

Composition:

	Resolving gel (12%)	Stacking gel (4%)
30% PAA	2ml	267 µl
4x resolving gel buffer	1.25ml	-
4x stacking gel buffer	-	500 µl
ddH <sub>2</sub> O	1.75ml	1233 µl
10% APS	60 µl	20 µl
TEMED	10 µl	5 µl

First the resolving gel was poured and covered with a layer of isopropanol to ensure a linear front between the resolving and the stacking gel. After removal of the isopropanol the stacking gel was poured on top of the resolving gel. APS and TEMED were always added as last components. 10 µl of each sample were applied per slot.

#### 2.2.4.4. Detection of proteins with Coomassie R250/G250

Coomassie is a dye that attaches basic amino acid side chains and therefore stains proteins unspecifically with a sensitivity of 0.05 to 0.1 µg per protein band.

---

The gel was stained for 30min by shaking at room temperature with Coomassie staining solution and then destained until the background was clear.

#### **2.2.4.5. Western blot analysis**

##### Semi dry transfer

The transfer of proteins on a membrane was performed by the electrophoretic semi-dry transfer.

Six sheets of 3MM Whatman paper and one sheet of nitrocellulose membrane were cut to the size of the gel and incubated in transblot buffer for several minutes. Afterwards the blot was assembled in the following order avoiding air bubbles:

1. anode
2. 3x 3MM Whatman paper
3. nitrocellulose membrane
4. gel
5. 3x 3MM Whatman paper
6. cathode

The gel was blotted at 20V for 20min (2 gels 30min).

##### Ponceau S staining of immobilised proteins

Ponceau S is a staining reagent that reversibly stains proteins immobilized on a nitrocellulose membrane. The membrane was incubated in Ponceau S solution until the protein bands became visible. The marker bands were marked before the membrane was destained with water.

---

### Antibody probing

After blotting of the proteins on the membrane unspecific binding sites were blocked with 5% milk powder in 1x TBS over night at 4°C by shaking.

The following steps are all performed at room temperature.

The blot was washed once with 1x TBS for 10min before 10ml of primary antibody solution were added for one hour. The blot was then washed three times with 1x TBS for 10min and incubated with 10ml of the secondary antibody solution for one hour. Three final washing steps with 1x TBS (10min) were performed afterwards. The blot was developed using the ECL kit form PIERCE and exposed onto a hyperfilm ECL obtainend by Amersham Biosciences.

---

## **2.3. Cloning strategies**

### **2.3.1. Construction of plasmids containing different fragments of the putative origin region of $\phi$ Ch1**

#### **2.3.1.1. Construction of pRo-1**

The fragment comprising nu. 34659-37592 of the  $\phi$ Ch1 DNA was amplified with the primers Ro1 and Ro2 restricted with *KpnI* and *HindIII* and introduced into pNov-1 restricted with the same enzymes.

#### **2.3.1.2. Construction of pRo-2**

The fragment comprising nu. 34659-37978 of the  $\phi$ Ch1 DNA was amplified with the primers Ro1 and Ro3 restricted with *KpnI* and *HindIII* and introduced into pNov-1 restricted with the same enzymes.

#### **2.3.1.3. Construction of pRo-3**

The plasmid pRo-5 was restricted with *SmaI* and *HindIII* and the remaining vector isolated. The fragment comprising nu. 36164-37978 of the  $\phi$ Ch1 DNA was amplified with the primers Ro6 and Ro3, restricted with *SmaI* and *HindIII* and introduced into a modified pRo-5 plasmid. The resulting plasmid pRo-3 contains the nu. 33953-34479 and 36164-37978 of the  $\phi$ Ch1 DNA.

---

#### **2.3.1.4. Construction of pRo-4**

The fragment comprising nu. 33952-37947 of the  $\phi$ Ch1 DNA was excised from the plasmid pKS<sub>II</sub><sup>+</sup> Ro5/Ro4 with the enzymes *Xba*I, *Kpn*I and *Dra*I and introduced into pNov-1.

#### **2.3.1.5. Construction of pRo-5**

The fragment comprising nu. 37765-36164 of the  $\phi$ Ch1 DNA was amplified with the primers Ro6 and TR4, restricted with *Sma*I and *Hind*III and introduced into pKS<sub>II</sub><sup>+</sup>. As a second step, the fragment comprising nu. 36164-34626 of the  $\phi$ Ch1 DNA was amplified with the primers Ro7 and TR3, restricted with *Sma*I and *Xba*I and introduced into the plasmid constructed in the first cloning step. In a third step, the fragment comprising nu. 339953-34479 of the  $\phi$ Ch1 DNA was amplified with the primers TR1 and TR2, restricted with *Not*I and *Xba*I and introduced into the plasmid containing the two earlier cloned fragments. Finally the resulting plasmid pKS<sub>II</sub><sup>+</sup> TR1/TR4 was restricted with *Not*I and *Hind*III. The TR1/TR4 fragment was isolated and introduced into the plasmid pNov-1.

#### **2.3.1.6. Construction of pRo-6**

The plasmid pRo-5 was restricted with *Sma*I and *Not*I and the remaining vector isolated. The *Not*I/*Sma*I fragment from the plasmid pRo-4 was isolated and introduced into the remaining pRo-5 vector. The resulting plasmid pRo-6 contains the nu. 33952-37765 of the  $\phi$ Ch1 DNA.

---

## **2.3.2. Construction of plasmids to analyse the function of the $\lambda$ -like integrase Int1**

### **2.3.2.1. Construction of pUC52-1**

Open reading frame 34 was cloned by amplification with the primers 34Kpn and 34-3Xba using the template pBgB52. The fragment was restricted with *KpnI* and *XbaI* and introduced into pUC19.

### **2.3.2.2. Construction of pRo-5 52-2**

Open reading frame 36 and int1 were amplified with the primers 36-51Xba and 36-5Hind using the template pBgB52. The fragment was restricted with *XbaI* and *HindIII* and introduced into pUC52-1 resulting in pUC52-2. As a final step the fragment including ORF34, ORF36 and int1 (ORF35) was isolated through restriction of pUC52-2 with *FspI* and *HindIII*. The *FspI/HindIII* fragment was then introduced into pRo-5,

### **2.3.2.3. Construction of pRo-5 52-3**

Open reading frame 36 was amplified with the primers 36-51Xba and 36-5Hind using the template pBgB52 $\Delta$ int1. The fragment was restricted with *XbaI* and *HindIII* and introduced into pUC52-1 resulting in pUC52-3. As a final step the whole fragment including ORF34 and ORF36 was isolated through restriction of pUC52-3 with *FspI* and *HindIII*. The *FspI/HindIII* fragment was then introduced into pRo-5.

---

#### **2.3.2.4. Construction of pBAD24-int1 (ORF35)**

Open reading frame 35 (nu. 24902-25593) was amplified with the primers JasInt5 and Int13Xba using  $\phi$ Ch1 DNA as template, restricted with *Nco*I and *Xba*I and introduced into pBAD24.

#### **2.3.2.5. Cloning of ORF28 IR-R-Xba/IR-L-Hind fragment into pBAD24-int1 resulting in the plasmid pIR-28-int1**

The ORF28 fragment was amplified with the primers IR-R-Xba and IR-L-Hind using pQE-ORF28 as a template, restricted with *Xba*I and *Hind*III and introduced into pBAD24-int1.

#### **2.3.2.6. Cloning of ORF28 DR-R-Xba/IR-L-Hind fragment into pBAD24-int1 resulting in the plasmid pDR-28-int1**

The ORF28 fragment was amplified with the primers DR-R-Xba and IR-L-Hind using pQE-ORF28 as a template, restricted with *Xba*I and *Hind*III and introduced into pBAD24-int1.

#### **2.3.2.7. Cloning of the point mutations in the repeat fragment of IR-R-Xba resulting in the plasmids pIRM1-28-int1, pIRM4-28-int1, pIRM7-28-int1 and pIRM11-28-int1**

The ORF28 fragment was amplified with the primers IR-M1/IR-M4/IR-M7/IR-M11 and IR-L-Hind using pQE-ORF28 as a template, restricted with *Xba*I and *Hind*III and introduced into pBAD24-int1.

---

#### 2.3.2.8. Construction of pIR<sub>17-28</sub>

The 3' repeat sequence was amplified with the primers A7 and A8 using the template pBgB1, restricted with *Pst*I and *Hind*III and introduced into pKS<sub>II</sub><sup>+</sup>, resulting in the plasmid pKSA7. As a second step the 5' repeat sequence was amplified with the primers 34-5 and A4 using the template pBgB1, restricted with *Bgl*II and *Sma*I and introduced into pKSA7, resulting in pKSA7-A4. Then the ORF28 fragment was amplified with the primers 28Sma and 28Pst, restricted with *Pst*I and introduced into pKSA7-A4. Finally the whole fragment was excised with *Xba*I, *Hind*III and *Dra*I and introduced into pBAD24-int1, resulting in pIR<sub>17-28</sub>.

#### 2.3.2.9. Construction of pIR<sub>16-28</sub>

The 3' repeat sequence was amplified with the primers A7 and A8 using the template pBgB1, restricted with *Pst*I and *Hind*III and introduced into pKS<sub>II</sub><sup>+</sup>, resulting in the plasmid pKSA7. As a second step the 5' repeat sequence was amplified with the primers 34-5 and A4k using the template pBgB1, restricted with *Bgl*II and *Sma*I and introduced into pKSA7, resulting in pKSA7-A4k. Then the ORF28 fragment was amplified with the primers 28Sma and 28Pst, restricted with *Pst*I and introduced into pKSA7-A4k. Finally the whole fragment was excised with *Xba*I, *Hind*III and *Dra*I and introduced into pBAD24-int1, resulting in pIR<sub>17-28</sub>.



---

## 3. Results and Discussion

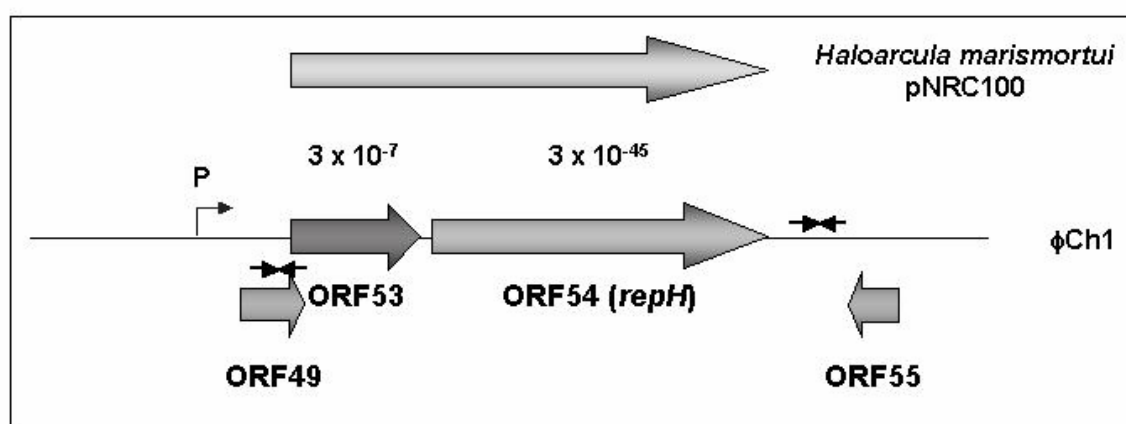
### 3.1. Establishment of a shuttle vector system for *Natrialba magadii*

Until now bacterial and haloarchaeal model systems were used (*E. coli* and *Hfx. volcanii*) for investigation of  $\phi$ Ch1 and *Nab. magadii*. With the establishment of a transformation system experiments could be performed in their natural environment, giving a better insight in these organisms.

#### 3.1.1. Development and analysis of different vectors

Sequence analysis of the minimal replication origin of halophilic plasmids showed the requirement for a unique gene, *repH*, and an AT-rich region 5' to the gene. Elimination of either the AT-rich sequence or the *repH* gene was found to abolish the autonomous replication ability of plasmids (Ng and DasSarma, 1993). Similarity searches using the  $\phi$ Ch1 DNA revealed an open reading frame with protein sequences of halophilic plasmids (Klein *et al.* 2002). ORF54, starting with GTG, encodes a large 581 aa protein with a calculated size of 65.2kDa and a pI of 4.8. The predicted protein shares similarities (highest similarity with BLASTP:  $5 \times 10^{-46}$ ) with archaeal proteins encoded by *Hal. marismortui* pNRC100, *Hbt. salinarum* plasmid pHH1, *Hbt. salinarum* p $\phi$ HL, *Halobacterium* sp. (strain NRC-1) pNRC100, and on *Haloferax volcanii* plasmid pHV2. Some of those proteins have been shown to be essential components of the minimal replicons of halophilic *Archaea* (Ng and DasSarma, 1993; Pfeifer and Ghahraman, 1993). However, none of the proteins shows sequence similarities to replication initiation proteins involved in either theta-type, strand displacement-type or rolling circle-type replication in bacteria (Del Solar *et al.*, 1998). An analysis of the deduced amino acid sequence of ORF54 with the program COILS revealed a putative coiled-coil domain located in the

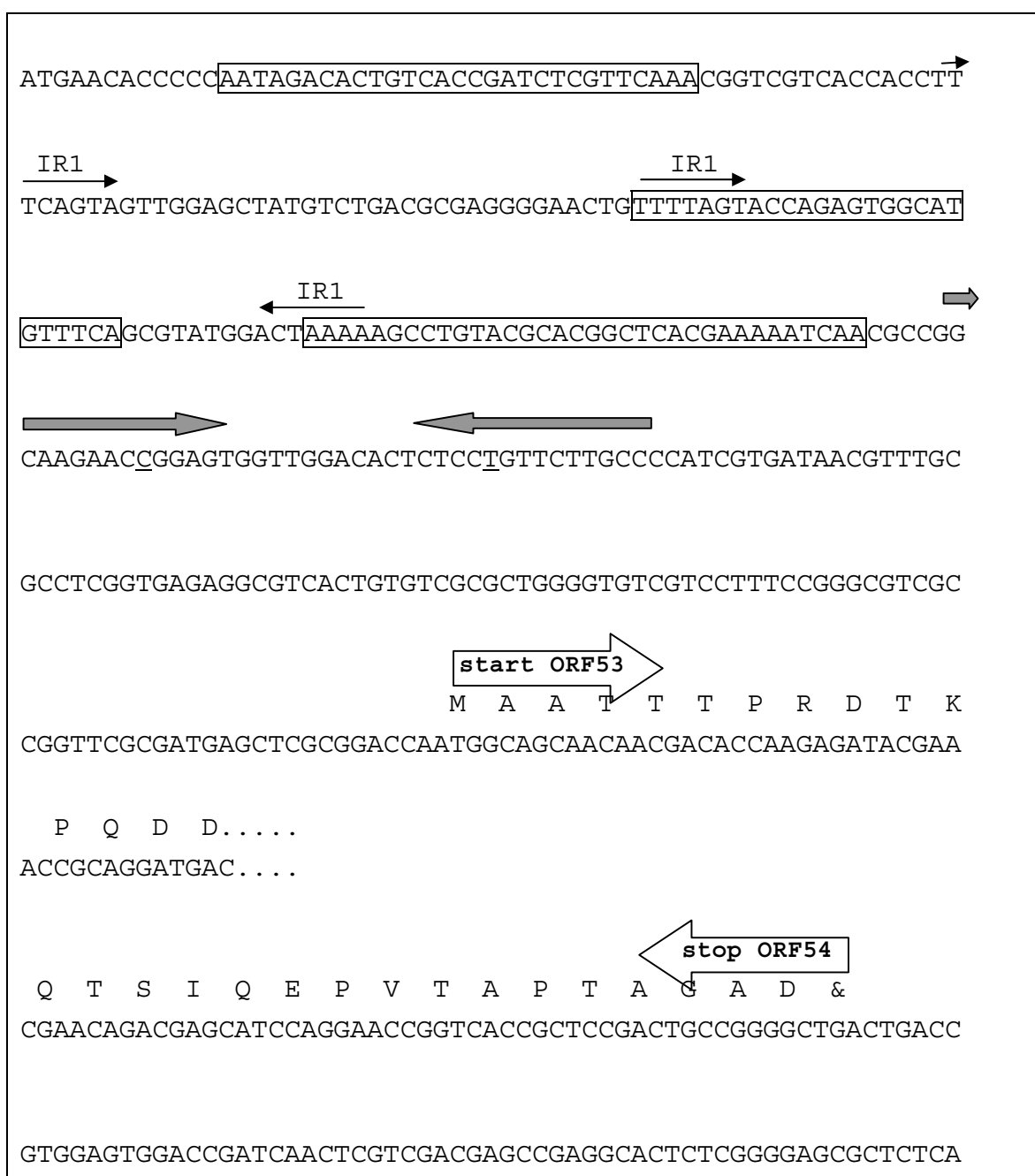
central part of the protein (amino acid residues 254-282). However, ORF54 is smaller in size as the homolog genes of known halophilic replication proteins and it resembles the C-terminal part of these proteins. ORF53, located upstream of ORF54, had a lower but significant similarity to the RepH protein encoded by *Hal. marismortui* pNRC100 (Figure 8). This similarity is restricted to the N-terminal part of RepH. Therefore, the putative replication protein of  $\phi$ Ch1 seemed to be composed of two different open reading frames.



**Figure 8: Presentation of the putative origin of replication of the virus  $\phi$ Ch1. Large arrows indicate ORF53 and ORF54 as well as ORF49 and ORF55. Sequence similarities of ORF53 and ORF54 to the pNRC100 replication protein H-like open reading frame of *Hal. marismortui* are indicated as well as the open reading frame. Arrows mark palindrome sequences. Lanes indicate the parts of the sequence cloned and the names of the different constructs are given on the right. The probe used for southern hybridization is indicated and marked.**

The same arrangement could be found within the genome of the nearest neighbor of  $\phi$ Ch1,  $\phi$ H infecting *Hbt. salinarum*. Again two different open reading frames could be identified with similarities to those proteins of halophilic *Archaea* necessary for autonomous replication of extra-chromosomal elements (data not shown). An AT rich region could also be detected within the upstream region of ORF53, and a second one in the downstream region of ORF54, suggesting promoter sequences. No such area could be seen in the 5'-region of ORF54, what leads to the suggestion that ORF53 and ORF54 are a transcriptional unit (Figure

9). The palindromic sequences as well as the repeat sequences, located upstream of ORF53 and downstream of ORF54, could be involved in the binding of proteins associated with replication (Figure 9) (Kornberg and Baker, 1992; Schnos *et al.*, 1988). Taken together, it seemed reasonable, that the region described above encodes a putative autonomous replication region. Therefore, this region was taken to develop a shuttle vector system for *E. coli/Nab. magadii*.



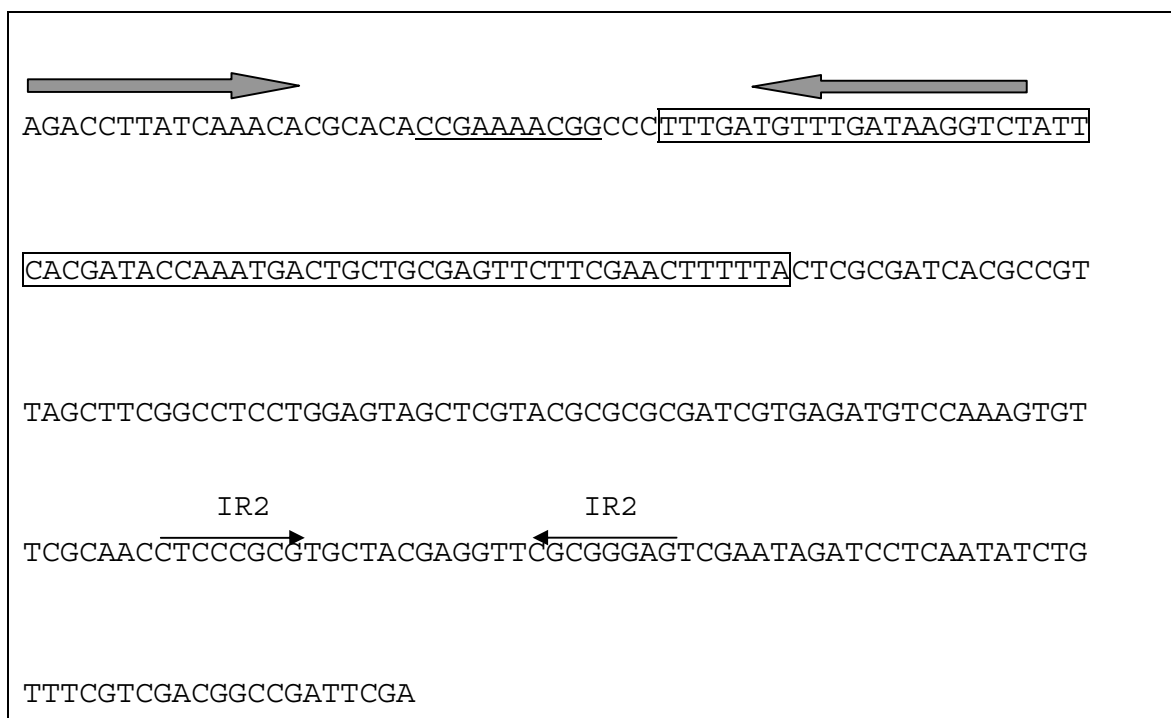


**Figure 9: The up- and downstream sequences of ORF53 and ORF54. A part of the central region of  $\phi$ Ch1 is given (nu. 34480-37901, accession number AF440695). Parts of the amino acid sequences of ORF53 and ORF54 are indicated by the one letter code and are given above the nucleotide sequence. White arrows indicate the start and stop of ORF53 and ORF54. AT rich regions (GC content of 42% or below) are framed. Palindromic sequences in the up- and downstream sequences are marked with arrows. Repeats are marked with arrows and indicated with IR1 and IR2.**

However the detailed function of the components of the  $\phi$ Ch1 replication origin is not discovered yet. Therefore several different variants of the replication origin of  $\phi$ Ch1 were cloned into the plasmid pNov-I (Figure 10A). Plasmid pNov-I was constructed by inserting the novobiocin resistance gene *gyrB* into pKS<sub>II</sub><sup>+</sup>. Novobiocin acts by inhibiting the DNA gyrase and can be used as a selective marker in halophilic *Archaea*.

Six different constructs were cloned in this way (Figure 10B and C) and were tested for their ability of autonomous replication in *Nab. magadii* L13.

The first construct pRo-1 contains only ORF53 and ORF54 (*repH*) without the upstream promoter region. Plasmid pRo-2 contains the promoter-less ORF53 and ORF54 as well as ORF55, including the palindromic sequences at the C-terminus.

As shown in Figure 13, pRo-1 and pRo-2 were not able to replicate in *Nab. magadii* L13.

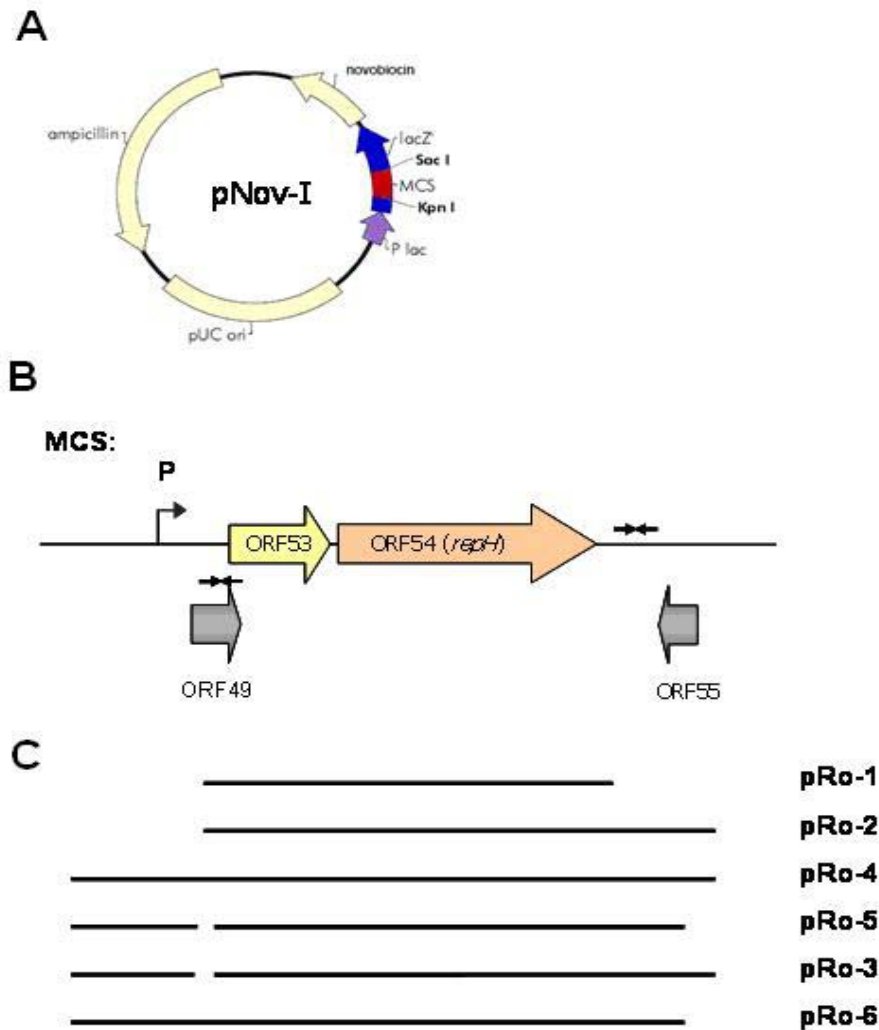


Figure 10: A: Schematic drawing of the vector pNov-I, that was used for construction of a shuttle vector system. B: Schematic drawing of the putative origin of replication of the  $\phi$ Ch1 genome that was cloned into the multiple cloning site (MCS) of pNov-I. Large arrows indicate ORF53, ORF54, ORF49 and ORF55. Small arrows mark palindromic sequences. P: promoter C: Drawing of the six cloned variants of the replication origin of  $\phi$ Ch1. The names of the constructs are given on the right.

---

The constructs made in the following all include the upstream promoter region, to ensure transcription.

The plasmid pRo-4 contains the whole sequence, starting at the promoter sequence upstream of ORF53 and ending at ORF55. Transformation was successful for this construct, but the efficiency was lowered in respect to pRo-3, pRo-5 and pRo-6 (Figure 13).

Sequence analysis of the  $\phi$ Ch1 genome identified ORF55 as putative transcriptional regulator, whereas no similarities were found for ORF49 (Klein *et al.*, 2002). But previous studies lead to the isolation of a  $\phi$ Ch1 population with a mutated form of ORF49 ( $\phi$ Ch1-1 and L11-1 respectively). A doubling of the upstream part of ORF49 and the 5' part of ORF49 itself leads to a changed lysis behaviour. In particular the onset of lysis occurs approximately two days earlier (Figure 11) (Iro *et al.*, 2006).

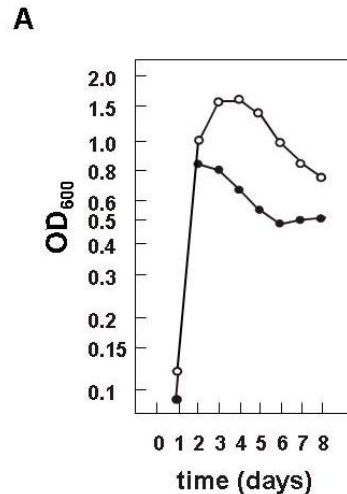


**Figure 11: The difference in lysis behavior of strains *Nab. magadii* L11 and L11-1 is the result of a short duplication within  $\phi$ Ch1-1. (A) Cells were grown for 8 days with aeration in rich medium. Measuring the optical density at 600 nm monitored growth and lysis of the cells.  $\circ$ , *Nab. magadii* L11;  $\bullet$ , *Nab. magadii* L11-1 (Iro *et al.*, 2006).**

An AT rich region is located upstream of ORF49 suggesting a promoter consensus sequence (Soppa *et al.*, 1999). ORF48 represses the transcription from this

promoter and is constitutively expressed throughout the whole life cycle of  $\phi$ Ch1. The expression of ORF49, however, is delayed in the lysogenic strain L11 but steadily increases during the virus life cycle until lysis (Figure 12). As mentioned in the introduction it is possible that RecA mediated self-cleavage is responsible for the abolishment of repression and induction of ORF49 expression (Iro *et al*, 2006).

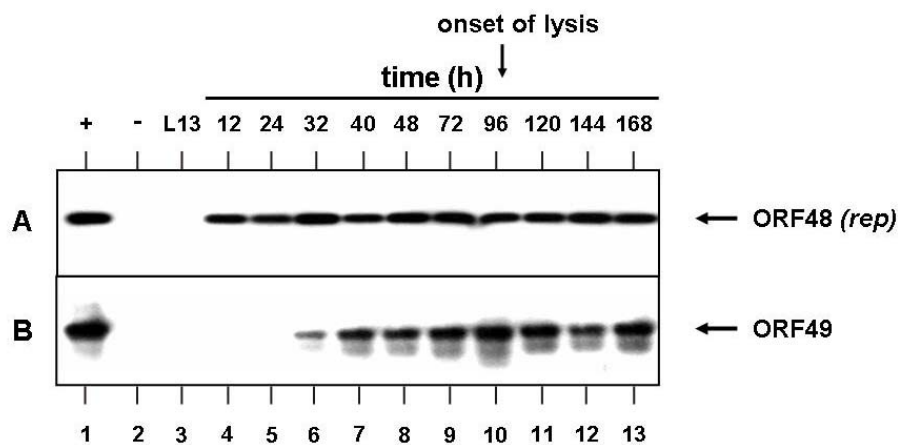


**Figure 12: Detection of  $\phi$ Ch1 *rep* and ORF49 gene transcripts during the life cycle of *Nab. magadii* L11 using RT-PCR. PCR and RT-PCR products from samples taken at various time points during the life cycle of  $\phi$ Ch1 in the lysogenic strain L11 were separated on 0.8% agarose gels. To confirm the fragments of the RT-PCR analysis, Southern hybridizations were performed with the *rep* or ORF49 fragment as a probe. (A) RT-PCRs of samples taken at different time points using *rep* gene specific primers BgL-3 and BgL-4. As a hybridization probe, the entire cloned *rep* gene fragment was used. (+), positive control: PCR using  $\phi$ Ch1 genomic DNA as a template; (-), negative control: PCR without a preceding RT-reaction using total RNA isolated from *Nab. magadii* L11 120h after inoculation; L13, RT-PCR using total RNA isolated from the virus-cured strain *Nab. magadii* L13; 12 - 168, RT-PCRs using samples taken at different time points (hours) after inoculation of *Nab. magadii* L11. (B) RT-PCRs using the ORF49 gene specific primers 49Ncol-5 and 49Ncol-3. As a hybridization probe, the entire cloned ORF49 gene fragment was used. Arrows indicate the products as well as the onset of lysis (Iro *et al*, 2006).**

Taken together ORF49 seems to be a regulator for the infection cycle of  $\phi$ Ch1.

Two of the variants of the putative  $\phi$ Ch1 origin of replication that were cloned into pNov-I (Figure 10C) contain ORF49 but they do not contain the putative repressor

---

ORF48, leading to a constitutive expression of ORF49. It cannot be excluded that ORF49 has an effect on the replication from this region.

In order to get more detailed information of the function of ORF49 and ORF55 three constructs were made. Plasmid pRo-3 lacks, in comparison to pRo-4, only the start-codon of ORF49, but contains the palindromic sequences embedded in ORF49. Plasmid pRo-6, in contrast, lacks the stop-codon of ORF55. To exclude a possible repression from both genes pRo-5 was constructed, lacking the start-codon of ORF49 and the stop-codon of ORF55 and therefore contains no putative repressor sequences (Figure 10C). All these constructs showed a suitable transformation efficiency of about  $10^3$  cfu/ $\mu$ g DNA (Figure 13).

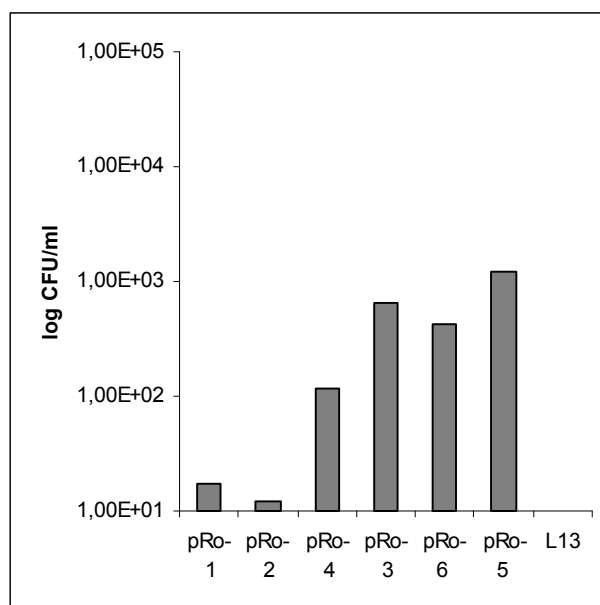


**Figure 13: Transformation efficiency of different constructs: the efficiency was quoted in colony forming units per ml (cfu/ml) on the left side and the clones used in this study are indicated at the bottom. For transformation 1 $\mu$ g of plasmid DNA was used.**

Furthermore phage titer assays with the previously made constructs were used to investigate an effect of ORF49 and ORF55 on the infectivity of  $\phi$ Ch1.

Therefore *Nab. magadii* (pRo-3), *Nab. magadii* (pRo-6) as well as *Nab. magadii* (pRo-5) were infected with  $\phi$ Ch1 (Figure 14A). Infection of  $\phi$ Ch1 was not impaired



when plated on strain *Nab. magadii* (pRo-3) and *Nab. magadii* (pRo-5) but completely abolished on strain *Nab. magadii* (pRo-6) (Figure 14B). Exact values are given in Table 2.

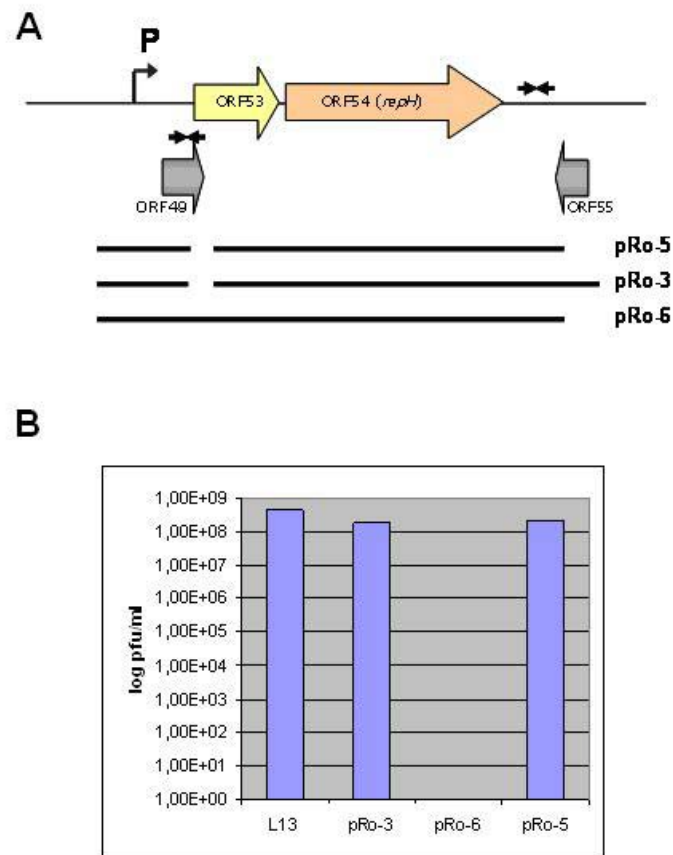


**Figure 14: A: Schematic drawing of the constructs containing or lacking putative repressors of the putative  $\phi$ Ch1 origin of replication used in phage titer assays. P: promoter B: Results of a phage titer assay: showing the effect of ORF49 on replication of phage  $\phi$ Ch1. pfu: plaque forming units**

This results lead to the suggestion, that ORF49 has its primary function in lysogeny like open reading frame 43, 44 and 48 (Meissner, 2008), as it applies complete immunity to infection, and not in regulation of the  $\phi$ Ch1 origin of replication.

ORF55, however, seems not to be involved in the regulation of the infection with  $\phi$ Ch1.

**Table 2: Titer [pfu/ml] and relative plating efficiency on L13 transformants expressing various transcripts schematically drawn in Figure 3A. Relative plating efficiency defined as phage titre on transformant relative to L13. Values are rounded to the nearest half-integer.**

strain	pfu/ml	relative plating efficiency
<i>Nab. magadii</i> L13	$4.6 \times 10^8$	1
<i>Nab. magadii</i> L13 (pRo-5)	$2.0 \times 10^8$	0.4
<i>Nab. magadii</i> L13 (pRo-3)	$1.9 \times 10^8$	0.4
<i>Nab. magadii</i> L13 (pRo-6)	$< 1 \times 10^1$	$< 1 \times 10^{-8}$

ORF48 is suggested to function as a repressor of the intergenic promoter region of ORF48 and ORF49 and therefore controls the expression of ORF49. Electrophoretic mobility shift assays showed that gp48 binds to this suggested promoter region (Meissner, 2008). Moreover phage titer assays with a strain carrying the plasmid pRo-5-ORF48 showed a reduction in infectivity of  $\phi$ Ch1 by three orders of magnitude (Meissner, 2008) whereas a reduction of eight orders of magnitude was observed for pRo-6. From this result it could be deduced that ORF49 is a stronger repressor for the lytic cycle than ORF48. However, the function of ORF48 seems to lie in the repression of ORF49 expression and not in the direct regulation of lysogeny.

The open reading frames 48 and 49 show different expression patterns in *Nab. magadii* L11 (Figure 12). Expression of ORF49 starts approximately sixty hours before onset of lysis and steadily increases whereas ORF48 is constitutively expressed.

---

Taken together these results lead to the suggestion that ORF49 functions as a repressor of superinfection. Therefore expression of ORF49, regulated by ORF48, would only be needed in the lytic stage of the virus life cycle.

As a next step phage titer assays with *Nab. magadii* (pRo-5) and the additionally cloned ORF49 have to be performed. This experiment would answer, whether ORF49 grants immunity to infection when it is expressed alone or only in pRo-6.

### **3.1.2. Characterization of *Nab. magadii* transformants**

Although the plasmids pRo-3, pRo-6 and pRo-5 all show a similar and suitable transformation rate for *Nab. magadii* L13 it was decided to use plasmid pRo-5 for further studies. The reason for this decision was that plasmid pRo-5 contains neither the putative repressor ORF49 nor the putative repressor ORF55 and therefore unknown effects from these two open reading frames can be avoided. A mutant of the virus containing an altered form of ORF49 showed an influence in  $\phi$ Ch1 gene development in previous studies (Iro *et al.*, 2006) and ORF55 shows similarities to known transcriptional regulators (Klein *et al.*, 2002).

The next step in characterization of the newly established transformation system was to determine the concentration dependence of the transformation efficiency. Therefore different amounts of plasmid pRo-5 were introduced into *Nab. magadii* L13 cells (Figure 15). The effect of different concentrations of the antibiotic novobiocin was also tested in this experiment. Transformation rates for 1.5  $\mu$ g/ml novobiocin seemed to be very nice, but further analyses showed that not every colony was successfully transformed and therefore contained no plasmid DNA (data not shown). Analyses of the colonies grown on 3  $\mu$ g/ml novobiocin plates showed no untransformed colonies. Therefore this novobiocin concentration was used in further studies as it was assured that cells only replicate in the presence of the plasmid pRo-5. Suitable transformation rates between  $10^3$  to  $10^4$  CFU/ml were reached for plasmid concentrations between 1  $\mu$ g and 10  $\mu$ g. However no

significant increase in transformation could be achieved from 5  $\mu\text{g}$  to 10  $\mu\text{g}$  DNA, due to possible precipitation of DNA in the transformation process.

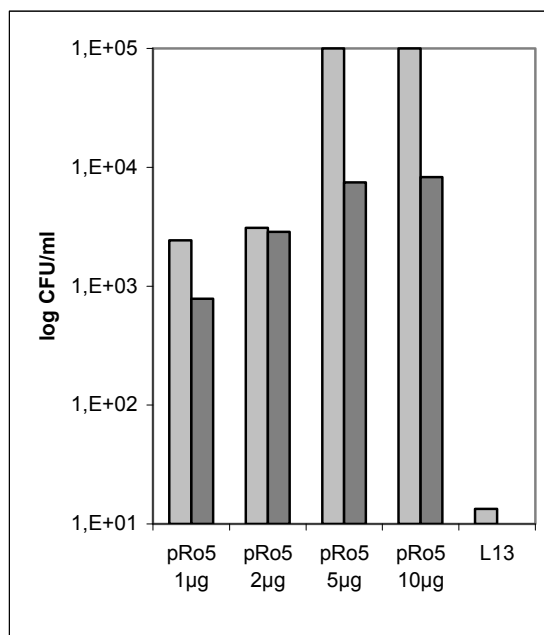


**Figure 15: Plasmid concentration dependant transformation efficiency of pRo-5. The light grey bars indicate 1.5  $\mu\text{g}/\text{ml}$  novobiocin and the dark grey bars 3  $\mu\text{g}/\text{ml}$  novobiocin containing plates. The efficiency was quoted in colony forming units per ml (cfu/ml) on the left side and the concentrations of plasmid pRo-5 used in this study are indicated at the bottom.**

To confirm that the transformants contain pRo-5, plasmid DNA was isolated (Figure 17A) and verified by PCR analysis with the primers TR1 and TR2, specific for the upstream promoter region of ORF53 and ORF54 (Figure 17C). All of the three tested cultures showed a positive result for the PCR.

In the following growth studies were performed with these three cultures of *Nab. magadii* L13 (pRo-5) resulting in the Arrhenius plots represented by Figure 16. Plasmid pRo-5 does not influence the growth of *Nab. magadii* L13 as the growth rates don't diverge greatly from the untransformed *Nab. magadii* L13 culture.

---

These results correlate with the determined plasmid copy number, which lies between one and five copies per *Nab. magadii* L13 cell.

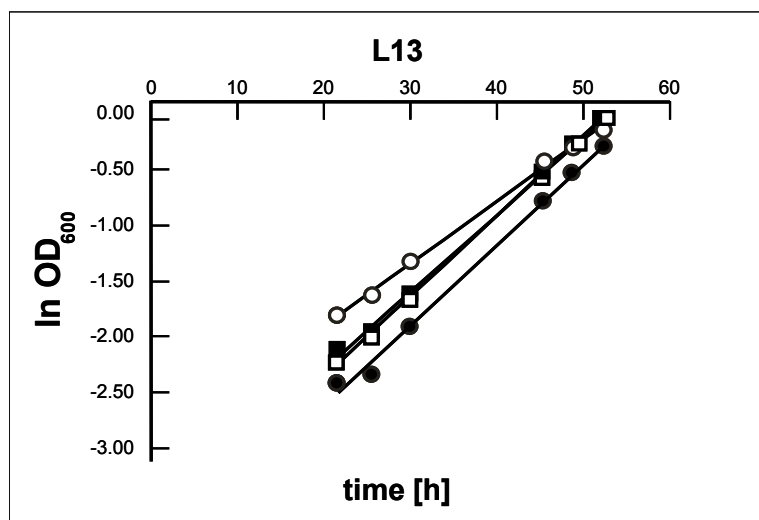


**Figure 16: Arrhenius plots for 3 different transformants of *Nab. magadii* L13 (pRo-5) and the untransformed strain: *Nab. magadii* L13 (○), *Nab. magadii* L13 (pRo-5<sub>1</sub>) (■), *Nab. magadii* L13 (pRo-5<sub>2</sub>) (□), *Nab. magadii* L13 (pRo-5<sub>3</sub>) (●). Cultures were grown in rich medium at 37°C with agitation. Novobiocin was added when required.**

To exclude an integration of plasmid pRo-5 into the *Nab. magadii* L13 genome southern hybridisation was performed. As a probe the upstream promoter region of ORF53 and ORF54 was used. Chromosomal DNA and plasmid DNA were isolated from three different *Nab. magadii* L13 (pRo-5) cultures and from *Nab. magadii* L13 (Figure 17A and B). Hybridisation could not be detected for *Nab. magadii* L13 (pRo-5) chromosomal DNA but was detected for *Nab. magadii* L13 (pRo-5) plasmid DNA. As expected the *Nab. magadii* L13 plasmid DNA and chromosomal DNA showed no hybridisation (Figure 17D). Therefore plasmid pRo-5 does not seem to integrate into the genome of *Nab. magadii* L13. Plasmid stability was determined by reintroducing plasmid pRo-5 isolated from *Nab. magadii* into *E. coli* and subsequent restriction analysis. Plasmid pRo-5 showed no rearrangements and variations and can therefore be assigned as stable (Iro *et al.*, in prep).

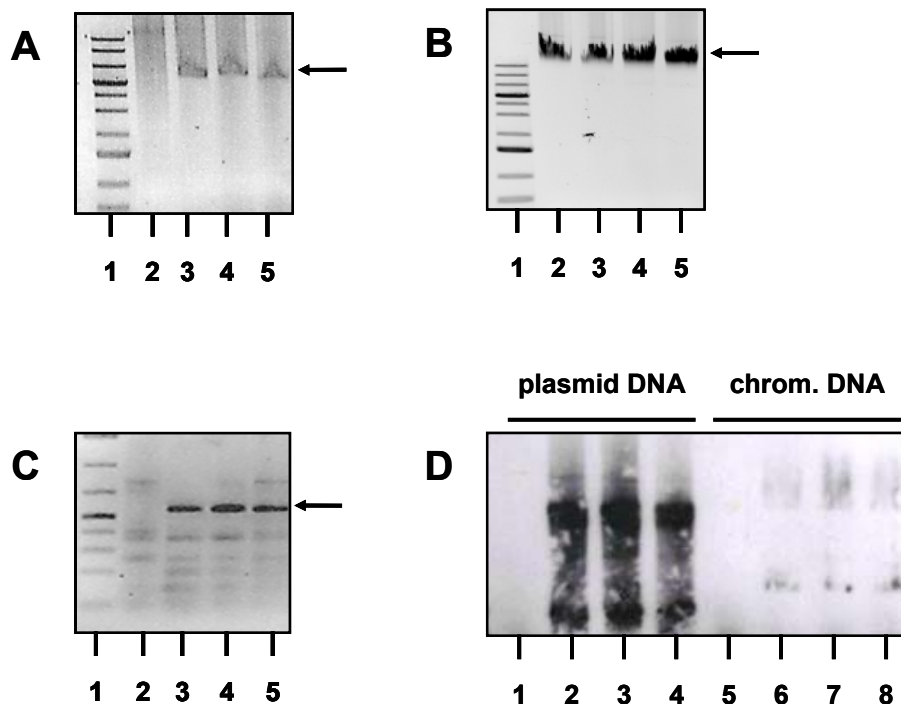
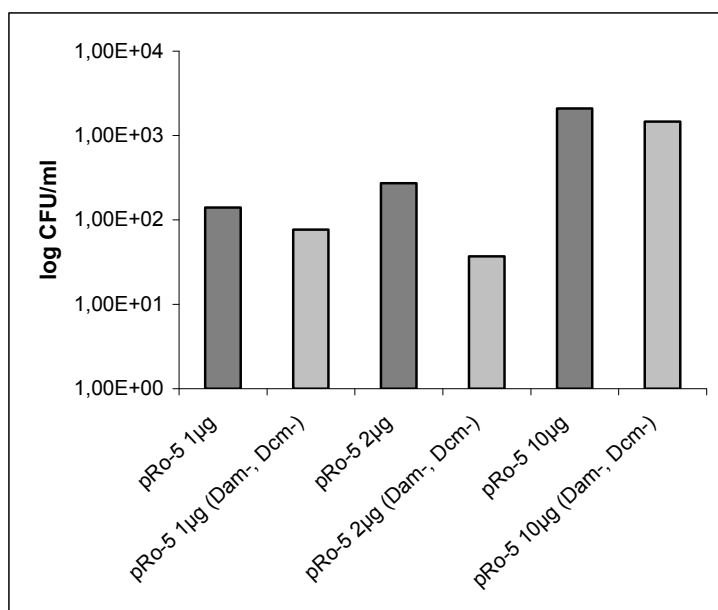


Figure 17: A: Plasmid isolation of transformed cells of *Nab. magadii* L13: lane 1: marker, lane 2: *Nab. magadii* L13, lanes 3-5: different cultures of *Nab. magadii* L13 (pRo-5). B: Isolation of chromosomal DNA of *Nab. magadii* L13: lane 1: marker, lane 2: *Nab. magadii* L13, lane 3-5: different cultures of *Nab. magadii* L13 (pRo-5). C: Isolated DNA preparations were analysed by PCR using primers specific for the promoter region of ORF53 and ORF54 (primers: TR1 and TR2). Lanes 1-5: same as in A. D: Southern hybridization of isolated DNA's (Fig 2 A, B) using the promoter sequence of ORF53 and ORF54 as probe. Lane 1 and 5: *Nab. magadii* L13, lanes 2-4 and 6-8: different cultures of *Nab. magadii* L13 (pRo-5).

Previously a higher transformation efficiency for unmethylated DNA in comparison to methylated DNA was published for *Hfx. volcanii* (Holmes *et al.*, 1991). This is due to the restriction-modification system in *Hfx. volcanii* that seems to degrade dam and dcm methylated DNA.

To investigate such a possible effect for *Nab. magadii* L13 unmethylated pRo-5 DNA was transformed. Therefore the *E. coli* strain JM110 was used, that is deficient in dam and dcm methylation. Plasmid DNA was isolated from this strain and transformed into *Nab. magadii* L13. Figure 18 compares the transformation rates of methylated and unmethylated plasmid pRo-5. For unmethylated DNA no

increase in transformation rates could be detected, actually a slight decrease is visible. This leads to the suggestion that *Nab. magadii* has a different restriction-modification system as *Hfx. volcanii* and transformation is independent on dam and dcm methylation.



**Figure 18: Comparison of the transformation efficiency of unmethylated plasmid pRo-5 (Dam<sup>-</sup>, Dcm<sup>-</sup>) and methylated plasmid pRo-5. The efficiency was quoted in colony forming units per ml (cfu/ml) on the left side and the concentrations of plasmid pRo-5 used in this study are indicated at the bottom.**

### **3.1.3. Transformation of different halophile and haloalkaliphile *Archaea***

To determine the host range of pRo-5, the plasmid was transformed in different halophilic and haloalkaliphilic *Archaea* (Table 3). The transformation protocol was adapted for the different strains, as described in Materials and Methods, section 1.3.

Successful transformation was established for the following strains: *Halorubrum saccharovorum*, *Hrr. coriense*, *Hrr. lacusprofundi*, *Hfx. volcanii* WFD11,

---

*Halobacterium salinarum* R1, *Natrialba asiatica* and *Natronobacterium gregorii*.

The putative origin of replication of  $\phi$ Ch1, therefore, can be used to introduce and maintain DNA in a variety of halophilic and haloalkaliphilic *Archaea*.

As a next step *Hfx. volcanii* WFD11 strain already transformed with pRo-5 was used to transform plasmid pMDS24 (Holmes and Dyll-Smith, 1999). These two plasmids contain different resistance markers to ensure selectivity. Co-transformation was successful leading to the suggestion that plasmid pMDS24 that contains a pHV2 originated origin of replication, seems to be in a different incompatibility group than the origin of replication of  $\phi$ Ch1 (Rawlings and Tietze, 2001).

**Table 3: Transformation of halo(alkali)philic *Archaea* with pRo-5**

---

strain	transformation
<i>Nab. magadii</i> L13	+
<i>Hrr. saccharovorum</i>	+
<i>Hrr. coriense</i>	+
<i>Hrr. lacusprofundi</i>	+
<i>Hfx. volcanii</i> WFD11	+
<i>Hfx. volcanii</i> WFD11 (pMDS24)	+
<i>Hbt. salinarum</i> R1	+
<i>Nab. asiatica</i>	+
<i>Nbt. gregorii</i>	+
<i>Hrr. sodomense</i>	-
<i>Nmn. pharaonis</i>	-

---

Additionally the stability of pRo-5 in *Hfx. volcanii* WFD11 was determined. Therefore plasmid DNA was isolated from *Hfx. volcanii* and transformed into *E. coli* XL1-Blue. Plasmid pRo-5 was then isolated from *E. coli* and restricted with *SacI*



---

what leads to a defined restriction pattern containing eight bands indicated on the left side of Figure 8. Ten different retransformed cultures were tested but only 50% showed the expected pattern (Figure 19). These results indicate that pRo-5 is quite instable in *Hfx. volcanii* WFD11 and undergoes rearrangements and variations in this host.

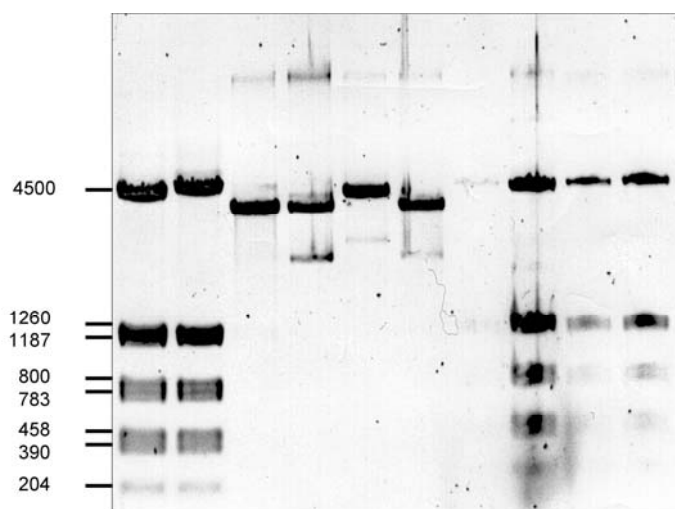


**Figure 19: Retransformation of *Hfx. volcanii* (pRo-5) into *E. coli* XL1-Blue.** The figure shows the digestion of the isolated plasmids with *SacI*. The numbers on the left side mark the expected bands after restriction.

When summarizing the results concerning the established pRo-5 shuttle vector system between *E. coli* and *Nab. magadii*, several points should be highlighted. The introduced plasmids have a copy number of 1 to 5 copies per *Nab. magadii* L13 cell and are quite stable. Furthermore, the plasmid seems not to integrate into the *Nab. magadii* genome. The host range of this system is also not limited to *Nab. magadii* as several different halophilic and haloalkaliphilic *Archaea* are transformable. Therefore pRo-5 seems to be a very promising tool for archaeal genetics and for the development of an inducible vector system for halo(alkali)philic *Archaea*.

---

### **3.2. The influence of *Int1* in the inversion reaction of $\phi$ Ch1**

The integrase *Int1*, encoded by ORF35 of the  $\phi$ Ch1 genome, is a member of the  $\lambda$ -integrase family of site-specific recombinases. Previous studies indicated the involvement of *Int1* in the variation of the putative tail fibre proteins encoded by ORF34 and ORF36 (Rössler *et al.*, 2002). The *int1* gene is surrounded by two repeat clusters (IR-L and IR-R) that are oriented in an inverted direction and embedded in ORF34 and ORF36. Inversion between these two clusters leads to exchange of the C-terminal parts of ORF34 and ORF36.

To investigate a possible involvement of *Int1* in the inversion reaction between the repeat clusters IR-L and IR-R several constructs were made.

#### **3.2.1. Analysis of single repeat constructs in *E. coli***

As a first step plasmids were constructed containing the *int1* gene and two single repeats separated by a spacer sequence. In one construct the repeats are oriented in an indirect direction similar to the original situation in the  $\phi$ Ch1 genome and in the other construct the repeats are oriented in a direct direction. Both constructs were introduced into the vector pBAD24, resulting in plasmids pIR-28-*int1* (with the indirect repeats) and pDR-28-*int1* (with the direct repeats) (Figure 20A). After transformation in *E. coli* XL1-Blue induction of *Int1* expression was achieved by addition of 0.2% L (+) arabinose (Figure 20B). PCR analyses with inversion specific primer sets were used to determine an inversion on DNA level (Figure 20C).

*Int1* seems to be only capable to invert the DNA if the repeats are in an inverted orientation, otherwise no inversion specific PCR product is detectable.

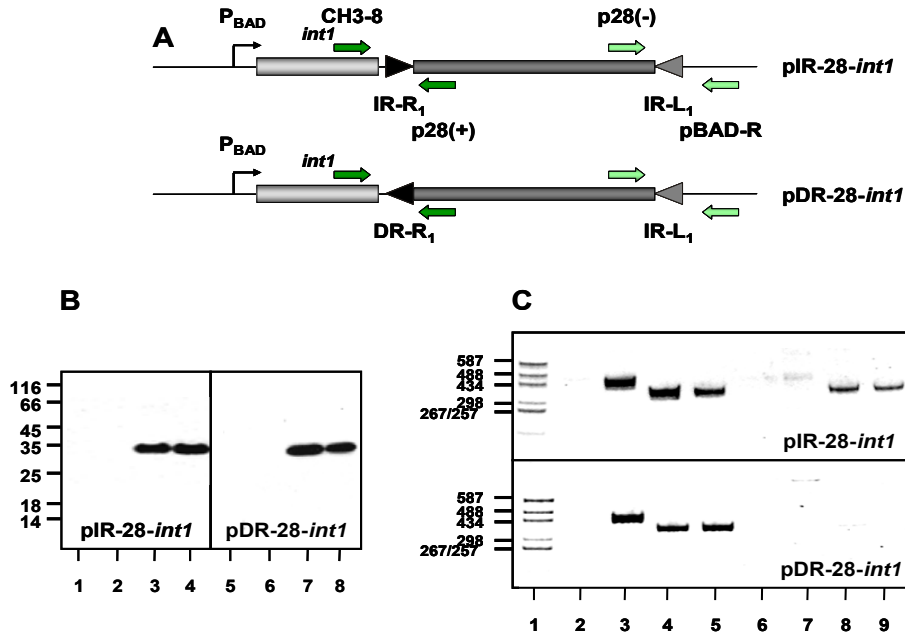


**Figure 20: Single repeat constructs:** **A:** Schematic representation of plasmids pIR-28-*int1* and pDR-28-*int1*. The *int1* gene is indicated as a light grey bar. An arrow indicates the promoter p<sub>BAD</sub> as well as its transcriptional direction. The repeats are marked with arrowheads. A dark grey bar indicates the spacer between two repeats. The position of primers CH3-8, p28(+), p28(-) and pBAD-R are marked with small arrows.

**B:** Expression of *int1*, induced by the addition of 0.02% L(+) arabinose was monitored in a western blot analysis using  $\alpha$ -His-Tag-antibodies. Crude extracts were prepared and total proteins were separated on a 12% PAA gel. Lane 1: XL1-Blue (pBAD24), induced for 2h with arabinose, lane 2: XL1-Blue (pBAD24), induced for 4h with arabinose, lane 3: XL1-Blue (pIR-28-*int1*), induced for 2h with arabinose, lane 4: XL1-Blue (pIR-28-*int1*), induced for 4h with arabinose, lane 5: XL1-Blue (pBAD24), induced for 2h with arabinose, lane 6: XL1-Blue (pBAD24), induced for 4h with arabinose, lane 7: XL1-Blue (pDR-28-*int1*), induced for 2h with arabinose, lane 8: XL1-Blue (pDR-28-*int1*), induced for 4h with arabinose.

**C:** PCR analysis to detect *in vivo* inversion. Plasmid DNA was isolated from the following cultures: upper panel: lane 2, 6: XL1-Blue (pBAD24), induced for 2h with arabinose, lane 3, 7: XL1-Blue (pBAD24), induced for 4h with arabinose, lane 4, 8: XL1-Blue (pIR-28-*int1*), induced for 2h with arabinose, lane 5, 9: XL1-Blue (pIR-28-*int1*), induced for 4h with arabinose; lower panel: lane 2, 6: XL1-Blue (pBAD24), induced for 2h with arabinose, lane 3, 7: XL1-Blue (pBAD24), induced for 4h with arabinose, lane 4, 8: XL1-Blue (pDR-28-*int1*), induced for 2h with arabinose, lane 5, 9: XL1-Blue (pDR-28-*int1*), induced for 4h with arabinose. PCR analyses with these DNA templates were performed with the following primer sets: lanes 2, 3, 6, 7: CH3-8 and pBAD-R, lanes 4, 5: CH3-8 and p28(+), lanes 8, 9: CH3-8 and p28(-), lane 1: size marker pUC19/*HaeIII*.

For further characterization of this inversion reaction it was decided to alter the wildtype IR-L repeat sequence in the pIR-28-*int1* construct and check for recombination. Table 3 shows the different IR-L sequences used. As a first step only the highly conserved region within the repeat clusters of ORF34 and ORF36 was tested, but recombination did not occur. It was suggested that the nine base pair conserved region is simple not able to allow binding of Int1. Therefore different point mutations within the conserved region were introduced into the wild type IR-L sequence (Table 4). Mutations at the third and fourth base did not influence the recombination event but mutations at the fifth and sixth base position prevented an inversion reaction. Binding at this specific site therefore seems to be very likely.

**Table 4: Different IR-L sequences and their ability for recombination**  
**Point mutations are marked in red. The conserved region is underlined.**

	Sequence	recombination
IR-WT	<u>ATGGACGCGG</u> TAAGTACGTCCGAGACGGCC	+
ΔIR	<u>ATGGACGCG</u>	-
IR-M1	<u>AT</u> <b>A</b> GACGCGGTAAGTACGTCCGAGACGGCC	+
IR-M4	<u>ATG</u> <b>A</b> ACGCGGTAAGTACGTCCGAGACGGCC	+
IR-M7	<u>ATGG</u> <b>T</b> CGCGGTAAGTACGTCCGAGACGGCC	-
IR-M11	<u>ATGGAA</u> <b>A</b> GCGGTAAGTACGTCCGAGACGGCC	-

### 3.2.2. Analysis of multiple repeat constructs in *E. coli*

In the  $\phi$ Ch1 genome the *int1* gene is not flanked by single repeats but by clusters of repeats, therefore the subsequent experiments were performed with repeat clusters (IR-L and IR-R). The two constructs pIR<sub>17-28</sub> and pIR<sub>16-28</sub> were built in a similar way than the single repeat constructs (Figure 21A). The two constructs differ in the IR-L repeat cluster, which contains a single overlapping reversed repeat in pIR<sub>17-28</sub> that is excluded in pIR<sub>16-28</sub>. Expression of Int1 was induced by

the addition of 0.2% L (+) arabinose (Figure 21B). PCR analysis of samples from different points in time before and after induction was performed with inversion specific primers (Figure 21C). For pIR<sub>17-28</sub> PCR analysis showed a product with the inversion specific primers after induction of gene expression, but for pIR<sub>16-28</sub> these primers give a product even if the *int1* gene is not expressed.

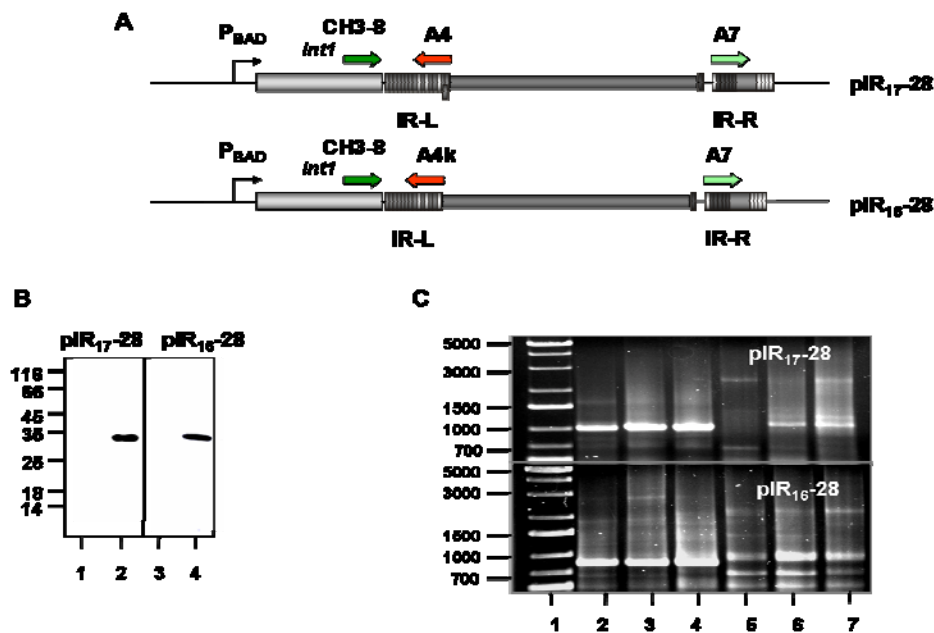


**Figure 21: Multiple repeat constructs:** A: Schematic representation of plasmids pIR<sub>17-28</sub> and pIR<sub>16-28</sub>. The *int1* gene is indicated as a light grey bar. An arrow indicates the promoter p<sub>BAD</sub> as well as its transcriptional direction. The repeats are organized in the clusters IR-L and IR-R and are displayed as small boxes. Repeats containing the conserved 5' end ATGGAcgC are indicated as dark grey boxes and repeats with mismatches within this sequence are marked with light grey boxes. Overlapping, reversed repeats within a cluster are drawn staggered and slightly lower with respect to the others. A dark grey bar indicates the spacer between the repeat clusters IR-L and IR-R. The position of primers CH3-8, A4, A4k and A7 are marked by small arrows.

**B:** Expression of *int1*, induced by the addition of 0.02% L (+) arabinose was monitored in a western blot analysis using  $\alpha$ -His-Tag-antibodies. Crude extracts were prepared and total proteins were separated on a 12% PAA gel. Lane 1: XL1-Blue (pIR<sub>17-28</sub>), not induced, lane 2: XL1-Blue (pIR<sub>17-28</sub>), induced for 2h with arabinose, lane 3: XL1-Blue (pIR<sub>16-28</sub>), not induced, lane 4: XL1-Blue (pIR<sub>16-28</sub>), induced for 2h with arabinose.

---

**C: PCR analysis to detect *in vivo* inversion. Plasmid DNA was isolated from the following cultures: upper panel: Lanes 2, 5: XL1-Blue (pIR<sub>17-28</sub>), not induced, lane 3, 6: XL1-Blue (pIR<sub>17-28</sub>), induced for 4h with arabinose, lane 4, 7: XL1-Blue (pIR<sub>17-28</sub>), induced for 6h with arabinose, lower panel: lane 1: marker, lane 2, 5: XL1-Blue (pIR<sub>16-28</sub>), not induced, lane 3, 6: XL1-Blue (pIR<sub>16-28</sub>), induced for 4h with arabinose, lane 4, 7: XL1-Blue (pIR<sub>16-28</sub>), induced for 6h with arabinose. PCR analyses with these DNAs were performed with the following primer sets: lanes 2, 3, 4: CH3-8 and A4 (upper panel) or A4k (lower panel), lanes 5, 6, 7: CH3-8 and A7. Lane 1: size marker 1kb DNA ladder (Fermentas).**

Therefore the 1000bp inversion band was isolated from an agarose gel and sequenced. Figure 22 shows the results obtained from sequencing. Although the inversion seems to take place without the expression of Int1, the 1000 bp DNA sequence contains only regions of ORF34 and ORF36. Analysis of the obtained sequences showed two different  $\phi$ Ch1 specific DNA regions that are in an inverted orientation to each other, indicating that an inversion reaction occurred at this site.

```
CTGAGAAGTACATCCGGATTTCCGGTGGCCGAACGAAGCGAGCTCTACTCGAGA
CTGAGAAGTACATCCGGATTTCCGGTGGCCGAACGAAGCGAGCTCTACTCGAGA
TCTACGGCTGATCGCGCCACTTCATCCTT -17bp spacer -
TCTACGGCTGATCGCGCCACTTCATCCTT
ATGAGTAAAATCTGGGAACCGAGCGGTGGCGTCGACGACAAGGTCTCTTTGGG
ATGAGTAAAATCTGGGAACCGAGCGGTGGCGTCGACGACAAGGTCTCTTTGGG
ATGTACCCCGAGGACCTCGACGCCCAGGATCGACAAGAAGTGTACGCTGAGGCG
ATGTACCCCGAGGACCTCGACGCCCAGGATCGACAAGAAGTGTACGCTGAGGCG
TTCGAGGATATCGTCAAGTCCTACTCGACGATGGCGACCGCCTGCCGGTATCAG
TTCGAGGATATCGTCAAGTCCTACTCGACGATGGCGACCGCCTGCCGGTATCAG
GCGATCATCGATGAGATGATCGACGACGAAACTCGAGCCCAGCTGATCGCTGAC
GCGATCATCGATGAGATGATCGACGACGAAACTCGAGCCCAGCTGATCGCTGAC
ACGCAGGCGGCGATGGAAGCGGTCAGTATCGCCCGACCGCGATGGACTCGATC
```

```

ACGCAGGCGGCGATGGAAGCGGTCAGTATCGCCCGACCGCGATGGACTCGATC
AGCGAGTCGTCCACAGCTATGGATCCGATCAGCGAGTCCATCGTCGCGATGGAG
AGCGAGTCGTCCACAGCTATGGATCCGATCAGCGAGTCCATCGTCGCGATGGAG
GCCGTGATCGATTTCGGACGATATCGCGCTCCCCGCTGTCGTCGAGAGCCAGATC
GCCGTGATCGATTTCGGACGATATCGCGCTCCCCGCTGTCGTCGAGAGCCAGATC
GCGATGGACGCG -20bp spacer-
GCGATGGACGCG
AATGGACGCGGTGAGCGACTCCCAGACGGCAATGGACGCGGTGAGCGACTCCCA
AATGGACGCGGTGAGCGACTCCCAGACGGCAATGGACGCGGTGAGCGACTCCCA
GACGGCA
GACGGCA
ATGGACGCGGTAAGTACGTCCGAGACGGCCATGGACGCGGTAAGTGCCTCCACC
ATGGACGCGGTAAGTACGTCCGAGACGGCCATGGACGCGGTAAGTGCCTCCACC
CTCGCGATGGATGCGATCTGGGATTCGCAGCTTGCTGGGACACCGTTGCTGCC
CTCGCGATGGATGCGATCTGGGATTCGCAGCTTGCTGGGACACCGTTGCTGCC
GTCTCGATGGCGGTTCGGGAAGTTTGTAGCCGCCAGAGCGGGCCTGG
GTCTCGATGGCGGTTCGGGAAGTTTGTAGCCGCCAGAGCGGGCCTGG

```

**Figure 22: Sequencing of the 1000bp inversion band from pIR<sub>16</sub>-28. Indicated in black is the  $\phi$ Ch1 genome sequence that matches the sequenced DNA. Indicated in red and in blue are the base pairs obtained by sequencing. The difference between the red and the blue sequence is the orientation in comparison to the  $\phi$ Ch1 genome, which is inverted.**

---

### 3.2.3. Analysis of Int1 in *Nab. magadii*

With the establishment of the pRo-5 shuttle vector system it was possible to investigate the influence of Int1 in the inversion reaction within the  $\phi$ Ch1 genome in its natural environment.

Therefore two constructs were made and introduced into pRo-5 (Figure 23A). The plasmid pRo-5 52-2 contains ORF34<sub>52</sub>, ORF35 and ORF36<sub>52</sub>, whereas plasmid pRo-5 52-3 differs only in the lacking *int1* gene. After successful transformation in *Nab. magadii* L13 a time course experiment was performed. At different time points indicated in Figure 23 samples were taken for PCR analysis and for expression analysis.

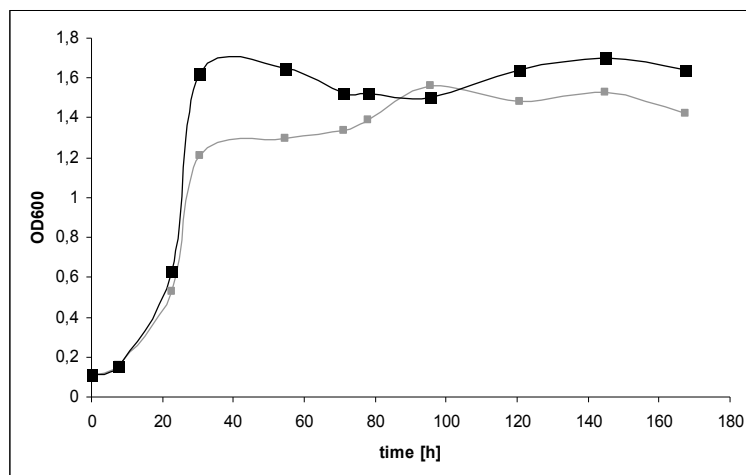


**Figure 23: Growth curve of *Nab. magadii* L13 (pRo-5 52-2) drawn in grey and *Nab. magadii* L13 (pRo-5 52-3) drawn in black. The squares indicate the points in time where samples were taken: 0h, 7.5h, 22.5h, 30.5h, 54.25h, 71h, 78h, 102.25h, 120.75h, 144.75h and 167.25h after inoculation.**

Expression of ORF34 was successfully monitored for both constructs indicated in Figure 24D and E. Strong expression of the protein could be observed between 71 and 78 h after inoculation of the strains, which is in the same range as ORF34 expression in the lysogenic strain (Rössler *et al.*, 2004). PCR amplification with



---

inversion specific primers was not successful for plasmid pRo-5 52-3 which does not contain the *int1* gene, but was successful for plasmid pRo-5 52-2. The PCR products obtained with inversion specific primers are detectable 78 hours after inoculation and are not very sharp (Figure 24B and C). This correlates to previous results, where five different variations of the invertible region within  $\phi$ Ch1 virus populations were found (Rössler *et al.*, 2004) (Figure 6). If the inversion reaction does not occur exactly between two corresponding repeats different numbers of repeats are obtained compared to the parental DNA. The length of the amplified DNA region therefore varies.

The fact that inversion is first detectable in the stationary growth phase of *Nab. magadii* L13 (pRo-5 52-2, pRo-5 52-3) did not correlate to the observation that *int1* expression was detected in the early logarithmic growth phase of the lysogenic strain *Nab. magadii* L11 (Rössler *et al.*, in prep). The differences seen in *int1* expression would suggest the interaction of a second protein, used for the early expression of *int1* in lysogenic strains. Here, a virus encoded protein could act as an activator of *int1*. Further experiments are needed to verify this assumption.

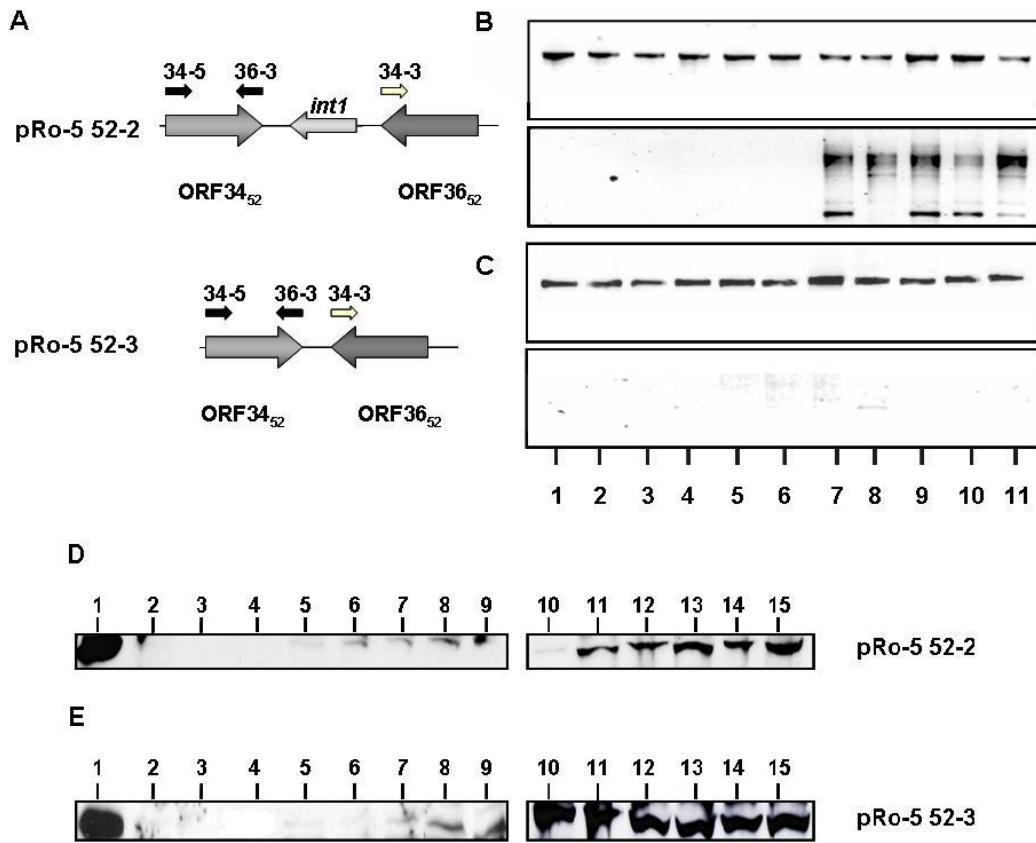


Figure 24: Analysis of *int1* in *Nab. magadii*: A: Schematic drawing of the constructs introduced in pRo-5. The big grey arrows indicate ORF34<sub>52</sub>, ORF36<sub>52</sub> and *int1*. The position of the primers 34-5, 36-3 and 34-3 are marked by small arrows.

B: PCR analysis to detect the inversion reaction *in vivo*.

Figure 12 shows the eleven points in time when samples were taken for PCR analysis (0h, 7.5h, 22.5h, 30.5h, 54.25h, 71h, 78h, 102.25h, 120.75h, 144.75h and 167.25h after inoculation).

Upper panel: Lane 1 to 11: *Nab. magadii* L13 (pRo-5 52-2) increasing points in time. For PCR analyses the primers 34-5 and 36-3 were used. Lower panel: Lane 1 to 11: *Nab. magadii* L13 (pRo-5 52-2) increasing points in time. For PCR analyses the primers 34-5 and 34-3 were used.

C: PCR analysis to detect the inversion reaction *in vivo*.

Figure 12 shows the eleven points in time when samples were taken for PCR analysis.

Upper panel: Lane 1 to 11: *Nab. magadii* L13 (pRo-5 52-3) increasing points in time. For PCR analyses the primers 34-5 and 36-3 were used. Lower panel: Lane 1 to 11: *Nab. magadii* L13 (pRo-5 52-3) increasing points in time. For PCR analyses the primers 34-5 and 34-3 were used.

---

**D: Expression of *int1* was monitored in a western blot analysis using  $\alpha$ -ORF36 antibodies. Crude extracts were prepared and total proteins were separated on a 12% PAA gel. Lane 1: XL1-Blue (ORF36 expression vector), lane 2: *Nab. magadii* L13, lane 3: *Nab. magadii* L13 (pRo-5), lane 4: empty, lane 5 to 15: *Nab. magadii* L13 (pRo-5 52-2) samples from the time experiment (0h, 7.5h, 22.5h, 30.5h, 54.25h, 71h, 78h, 102.25h, 120.75h, 144.75h and 167.25h after inoculation).**

**E: Expression of ORF34<sub>52</sub> was monitored in a western blot analysis using  $\alpha$ -ORF36 antibodies. Crude extracts were prepared and total proteins were separated on a 12% PAA gel. Upper pane: Lane 1: XL1-Blue (ORF36 expression vector), lane 2: *Nab. magadii* L13, lane 3: *Nab. magadii* L13 (pRo-5), lane 4: empty, lane 5 to 9: *Nab. magadii* L13 (pRo-5 52-3) first five samples from the time experiment (0h, 7.5h, 22.5h, 30.5h, 54.25h, 71h, 78h, 102.25h, 120.75h, 144.75h and 167.25h after inoculation).**

Concluding the previous results concerning the influence of *Int1* in the inversion reaction within the  $\phi$ Ch1 genome several aspects seem to be remarkable. The  $\lambda$ -like integrase *Int1* seems to be responsible for the inversion reaction between indirect repeat sequences. The inversion seems to be independent on the number of repeats as inversion products were obtained with single inverted repeats and with clusters of repeats. It was also possible to show an inversion not only in the *E. coli* model system but also in *Nab. magadii*, the original system. Taken together these results give a further hint to the function of *Int1* in the infection process of  $\phi$ Ch1.

---

## 4. Index of Figures and Tables

- Figure 1: Cell envelopes of an archaeon and a Gram-negative bacterium in a near-to-life state as obtained by cryo-electron tomography. (A) Section through the tomogram of an ice-embedded cell of *Pyrodictium abyssi*. The S-layer (SL) is anchored via long stalks in the cell membrane (CM) and defines the quasi-periplasmic space of the cell wall. The cytoplasmic density is removed. (B) A corresponding tomographic section through an ice-embedded cell of *Escherichia coli*, showing the cell envelope with the cell membrane (CM), the peptidoglycan (PG) and the outer membrane (OM). Note the considerable distance between the cell membrane and the peptidoglycan (Engelhardt, 2007)..... 12
- Figure 2: Electron micrograph of the wild type *Nab. magadii* L11, which carries  $\phi$ Ch1 as its prophage (left picture) and the indicator strain of *Nab. magadii*, L13 (right picture)..... 15
- Figure 3: Growth and lysis curve of *Nab. magadii* L11 (●). After the cells reach the stationary phase lysis starts. (○) Indicates the release of viruses into the medium. .... 16
- Figure 4: Electron micrograph of a  $\phi$ Ch1 particle negatively stained with uranyl acetate. The head shows an icosahedral structure and the contractile tail covers the shaft..... 17
- Figure 5: Linear representation of the 58498 bp virus  $\phi$ Ch1 genome starting at the *pac* site. ORFs are represented by arrows and numbered. Putative and verified functions of predicted gene products are indicated. The colors of the arrows indicate the frames of the ORFs: dark gray = 3<sup>rd</sup> reading frame, middle gray = 2<sup>nd</sup> reading frame and dark gray = 1<sup>st</sup> reading frame for both orientations..... 18
- Figure 6: The invertible region of  $\phi$ Ch1: Inversion exchanges the 3'ends of the open reading frames 34 and 36. The open reading frames of the integrase as well as the flanking open reading frames are indicated by arrows. .... 25

---

Figure 7: The invertible region of  $\phi$ Ch1. A: Growth and lysis of a lysogenic strain of *Nab. magadii*. Vertical asterisks indicate the time points of sample collection B: Time kinetics of the inversion reaction. Cell extracts were taken at different time points and used for PCR analysis to amplify ORF34. Primers used were (i) 34-5 and 34-3, in order to amplify ORF34 of the (+) segment (lanes 2 – 7) or (ii) 34-5 and 36-3, in order to amplify ORF34 of the (-) segment with the exchanged C-terminus (lanes 8 - 13). ..... 25

Figure 8: Presentation of the putative origin of replication of the virus  $\phi$ Ch1. Large arrows indicate ORF53 and ORF54 as well as ORF49 and ORF55. Sequence similarities of ORF53 and ORF54 to the pNRC100 replication protein H-like open reading frame of *Hal. marismortui* are indicated as well as the open reading frame. Arrows mark palindrome sequences. Lanes indicate the parts of the sequence cloned and the names of the different constructs are given on the right. The probe used for southern hybridization is indicated and marked. .... 58

Figure 9: The up- and downstream sequences of ORF53 and ORF54. A part of the central region of  $\phi$ Ch1 is given (nu. 34480-37901, accession number AF440695). Parts of the amino acid sequences of ORF53 and ORF54 are indicated by the one letter code and are given above the nucleotide sequence. White arrows indicate the start and stop of ORF53 and ORF54. AT rich regions (GC content of 42% or below) are framed. Palindromic sequences in the up- and downstream sequences are marked with arrows. Repeats are marked with arrows and indicated with IR1 and IR2. .... 60

Figure 10: A: Schematic drawing of the vector pNov-I, that was used for construction of a shuttle vector system. B: Schematic drawing of the putative origin of replication of the  $\phi$ Ch1 genome that was cloned into the multiple cloning site (MCS) of pNov-I. Large arrows indicate ORF53, ORF54, ORF49 and ORF55. Small arrows mark palindromic sequences. P: promoter C: Drawing of the six cloned variants of the replication origin of  $\phi$ Ch1. The names of the constructs are given on the right. .... 61

Figure 11: The difference in lysis behavior of strains *Nab. magadii* L11 and L11-1 is the result of a short duplication within  $\phi$ Ch1-1. (A) Cells were grown for 8 days

---

with aeration in rich medium. Measuring the optical density at 600 nm monitored growth and lysis of the cells. ○, *Nab. magadii* L11; ●, *Nab. magadii* L11-1 (Iro *et al*, 2006)..... 62

Figure 12: Detection of  $\phi$ Ch1 *rep* and ORF49 gene transcripts during the life cycle of *Nab. magadii* L11 using RT-PCR. PCR and RT-PCR products from samples taken at various time points during the life cycle of  $\phi$ Ch1 in the lysogenic strain L11 were separated on 0.8% agarose gels. To confirm the fragments of the RT-PCR analysis, Southern hybridizations were performed with the *rep* or ORF49 fragment as a probe. (A) RT-PCRs of samples taken at different time points using *rep* gene specific primers BgL-3 and BgL-4. As a hybridization probe, the entire cloned *rep* gene fragment was used. (+), positive control: PCR using  $\phi$ Ch1 genomic DNA as a template; (-), negative control: PCR without a preceding RT-reaction using total RNA isolated from *Nab. magadii* L11 120h after inoculation; L13, RT-PCR using total RNA isolated from the virus-cured strain *Nab. magadii* L13; 12 - 168, RT-PCRs using samples taken at different time points (hours) after inoculation of *Nab. magadii* L11. (B) RT-PCRs using the ORF49 gene specific primers 49Ncol-5 and 49Ncol-3. As a hybridization probe, the entire cloned ORF49 gene fragment was used. Arrows indicate the products as well as the onset of lysis (Iro *et al*, 2006)..... 63

Figure 13: Transformation efficiency of different constructs: the efficiency was quoted in colony forming units per ml (cfu/ml) on the left side and the clones used in this study are indicated at the bottom. For transformation 1 $\mu$ g of plasmid DNA was used. .... 64

Figure 14: A: Schematic drawing of the constructs containing or lacking putative repressors of the putative  $\phi$ Ch1 origin of replication used in phage titer assays. P: promoter B: Results of a phage titer assay: showing the effect of ORF49 on replication of phage  $\phi$ Ch1. pfu: plaque forming units ..... 65

Figure 15: Plasmid concentration dependant transformation efficiency of pRo-5. The light grey bars indicate 1.5  $\mu$ g/ml novobiocin and the dark grey bars 3  $\mu$ g/ml novobiocin containing plates. The efficiency was quoted in colony forming units per ml (cfu/ml) on the left side and the concentrations of plasmid pRo-5 used in this study are indicated at the bottom. .... 68

- 
- Figure 16: Arrhenius plots for 3 different transformants of *Nab. magadii* L13 (pRo-5) and the untransformed strain: *Nab. magadii* L13 (O), *Nab. magadii* L13 (pRo-5<sub>1</sub>) (■), *Nab. magadii* L13 (pRo-5<sub>2</sub>) (□), *Nab. magadii* L13 (pRo-5-5<sub>3</sub>) (●). Cultures were grown in rich medium at 37°C with agitation. Novobiocin was added when required. .... 69
- Figure 17: A: Plasmid isolation of transformed cells of *Nab. magadii* L13: lane 1: marker, lane 2: *Nab. magadii* L13, lanes 3-5: different cultures of *Nab. magadii* L13 (pRo-5). B: Isolation of chromosomal DNA of *Nab. magadii* L13: lane 1: marker, lane 2: *Nab. magadii* L13, lane 3-5: different cultures of *Nab. magadii* L13 (pRo-5). C: Isolated DNA preparations were analysed by PCR using primers specific for the promoter region of ORF53 and ORF54 (primers: TR1 and TR2). Lanes 1-5: same as in A. D: Southern hybridization of isolated DNA's (Fig 2 A, B) using the promoter sequence of ORF53 and ORF54 as probe. Lane 1 and 5: *Nab. magadii* L13, lanes 2-4 and 6-8: different cultures of *Nab. magadii* L13 (pRo-5). .... 70
- Figure 18: Comparison of the transformation efficiency of unmethylated plasmid pRo-5 (Dam-, Dcm-) and methylated plasmid pRo-5. The efficiency was quoted in colony forming units per ml (cfu/ml) on the left side and the concentrations of plasmid pRo-5 used in this study are indicated at the bottom. .... 71
- Figure 19: Retransformation of *Hfx. volcanii* (pRo-5) into *E. coli* XL1-Blue. The figure shows the digestion of the isolated plasmids with SacI. The numbers on the left side mark the expected bands after restriction. .... 73
- Figure 20: Single repeat constructs: A: Schematic representation of plasmids pIR-28-*int1* and pDR-28-*int1*. The *int1* gene is indicated as a light grey bar. An arrow indicates the promoter p<sub>BAD</sub> as well as its transcriptional direction. The repeats are marked with arrowheads. A dark grey bar indicates the spacer between two repeats. The position of primers CH3-8, p28(+), p28(-) and pBAD-R are marked with small arrows. B: Expression of *int1*, induced by the addition of 0.02% L(+) arabinose was monitored in a western blot analysis using □-His-Tag-antibodies. Crude extracts were prepared and total proteins were separated on a 12% PAA gel. Lane 1: XL1-Blue (pBAD24), induced for

2h with arabinose, lane 2: XL1-Blue (pBAD24), induced for 4h with arabinose, lane 3: XL1-Blue (pIR-28-*int1*), induced for 2h with arabinose, lane 4: XL1-Blue (pIR-28-*int1*), induced for 4h with arabinose, lane 5: XL1-Blue (pBAD24), induced for 2h with arabinose, lane 6: XL1-Blue (pBAD24), induced for 4h with arabinose, lane 7: XL1-Blue (pDR-28-*int1*), induced for 2h with arabinose, lane 8: XL1-Blue (pDR-28-*int1*), induced for 4h with arabinose. C: PCR analysis to detect *in vivo* inversion. Plasmid DNA was isolated from the following cultures: upper panel: lane 2, 6: XL1-Blue (pBAD24), induced for 2h with arabinose, lane 3, 7: XL1-Blue (pBAD24), induced for 4h with arabinose, lane 4, 8: XL1-Blue (pIR-28-*int1*), induced for 2h with arabinose, lane 5, 9: XL1-Blue (pIR-28-*int1*), induced for 4h with arabinose; lower panel: lane 2, 6: XL1-Blue (pBAD24), induced for 2h with arabinose, lane 3, 7: XL1-Blue (pBAD24), induced for 4h with arabinose, lane 4, 8: XL1-Blue (pDR-28-*int1*), induced for 2h with arabinose, lane 5, 9: XL1-Blue (pDR-28-*int1*), induced for 4h with arabinose. PCR analyses with these DNA templates were performed with the following primer sets: lanes 2, 3, 6, 7: CH3-8 and pBAD-R, lanes 4, 5: CH3-8 and p28(+), lanes 8, 9: CH3-8 and p28(-), lane 1: size marker pUC19/*HaeIII*.

..... 75

Figure 21: Multiple repeat constructs: A: Schematic representation of plasmids pIR<sub>17</sub>-28 and pIR<sub>16</sub>-28. The *int1* gene is indicated as a light grey bar. An arrow indicates the promoter p<sub>BAD</sub> as well as its transcriptional direction. The repeats are organized in the clusters IR-L and IR-R and are displayed as small boxes. Repeats containing the conserved 5' end ATGGAcgC are indicated as dark grey boxes and repeats with mismatches within this sequence are marked with light grey boxes. Overlapping, reversed repeats within a cluster are drawn staggered and slightly lower with respect to the others. A dark grey bar indicates the spacer between the repeat clusters IR-L and IR-R. The position of primers CH3-8, A4, A4k and A7 are marked by small arrows. B: Expression of *int1*, induced by the addition of 0.02% L (+) arabinose was monitored in a western blot analysis using □-His-Tag-antibodies. Crude extracts were prepared and total proteins were separated



on a 12% PAA gel. Lane 1: XL1-Blue (pIR<sub>17-28</sub>), not induced, lane 2: XL1-Blue (pIR<sub>17-28</sub>), induced for 2h with arabinose, lane 3: XL1-Blue (pIR<sub>16-28</sub>), not induced, lane 4: XL1-Blue (pIR<sub>16-28</sub>), induced for 2h with arabinose. C: PCR analysis to detect *in vivo* inversion. Plasmid DNA was isolated from the following cultures: upper panel: Lanes 2, 5: XL1-Blue (pIR<sub>17-28</sub>), not induced, lane 3, 6: XL1-Blue (pIR<sub>17-28</sub>), induced for 4h with arabinose, lane 4, 7: XL1-Blue (pIR<sub>17-28</sub>), induced for 6h with arabinose, lower panel: lane 1: marker, lane 2, 5: XL1-Blue (pIR<sub>16-28</sub>), not induced, lane 3, 6: XL1-Blue (pIR<sub>16-28</sub>), induced for 4h with arabinose, lane 4, 7: XL1-Blue (pIR<sub>16-28</sub>), induced for 6h with arabinose. PCR analyses with these DNAs were performed with the following primer sets: lanes 2, 3, 4: CH3-8 and A4 (upper panel) or A4k (lower panel), lanes 5, 6, 7: CH3-8 and A7. Lane 1: size marker 1kb DNA ladder (Fermentas).

..... 77

Figure 22: Sequencing of the 1000bp inversion band from pIR<sub>16-28</sub>. Indicated in black is the  $\phi$ Ch1 genome sequence that matches the sequenced DNA. Indicated in red and in blue are the base pairs obtained by sequencing. The difference between the red and the blue sequence is the orientation in comparison to the  $\phi$ Ch1 genome, which is inverted. .... 79

Figure 23: Growth curve of *Nab. magadii* L13 (pRo-5 52-2) drawn in grey and *Nab. magadii* L13 (pRo-5 52-3) drawn in black. The squares indicate the points in time where samples were taken: 0h, 7.5h, 22.5h, 30.5h, 54.25h, 71h, 78h, 102.25h, 120.75h, 144.75h and 167.25h after inoculation. .... 80

Figure 24: Analysis of *int1* in *Nab. magadii*: A: Schematic drawing of the constructs introduced in pRo-5. The big grey arrows indicate ORF34<sub>52</sub>, ORF36<sub>52</sub> and *int1*. The position of the primers 34-5, 36-3 and 34-3 are marked by small arrows. the primers 34-5, 36-3 and 34-3 are marked by small arrows. B: PCR analysis to detect the inversion reaction *in vivo*. Figure 12 shows the eleven points in time when samples were taken for PCR analysis (0h, 7.5h, 22.5h, 30.5h, 54.25h, 71h, 78h, 102.25h, 120.75h, 144.75h and 167.25h after inoculation). Upper panel: Lane 1 to 11: *Nab. magadii* L13 (pRo-5 52-2) increasing points in time. For PCR analyses the primers 34-5 and 36-3 were

used. Lower panel: Lane 1 to 11: *Nab. magadii* L13 (pRo-5 52-2) increasing points in time. For PCR analyses the primers 34-5 and 34-3 were used. C: PCR analysis to detect the inversion reaction *in vivo*. Figure 12 shows the eleven points in time when samples were taken for PCR analysis. Upper panel: Lane 1 to 11: *Nab. magadii* L13 (pRo-5 52-3) increasing points in time. For PCR analyses the primers 34-5 and 36-3 were used. Lower panel: Lane 1 to 11: *Nab. magadii* L13 (pRo-5 52-3) increasing points in time. For PCR analyses the primers 34-5 and 34-3 were used. D: Expression of int1 was monitored in a western blot analysis using  $\alpha$ -ORF36 antibodies. Crude extracts were prepared and total proteins were separated on a 12% PAA gel. Lane 1: XL1-Blue (ORF36 expression vector), lane 2: *Nab. magadii* L13, lane 3: *Nab. magadii* L13 (pRo-5), lane 4: empty, lane 5 to 15: *Nab. magadii* L13 (pRo-5 52-2) samples from the time experiment (0h, 7.5h, 22.5h, 30.5h, 54.25h, 71h, 78h, 102.25h, 120.75h, 144.75h and 167.25h after inoculation). E: Expression of ORF34<sub>52</sub> was monitored in a western blot analysis using  $\alpha$ -ORF36 antibodies. Crude extracts were prepared and total proteins were separated on a 12% PAA gel. Upper pane: Lane 1: XL1-Blue (ORF36 expression vector), lane 2: *Nab. magadii* L13, lane 3: *Nab. magadii* L13 (pRo-5), lane 4: empty, lane 5 to 9: *Nab. magadii* L13 (pRo-5 52-3) first five samples from the time experiment (0h, 7.5h, 22.5h, 30.5h, 54.25h, 71h, 78h, 102.25h, 120.75h, 144.75h and 167.25h after inoculation).

..... 82

Table 1: Number of repeats within proteins encoded by ORF34 and ORF36 and derivatives (Rössler <i>et al.</i> , 2004).....	23
Table 2: Titer [pfu/ml] and relative plating efficiency on L13 transformants expressing various transcripts schematically drawn in Figure 3A. Relative plating efficiency defined as phage titre on transformant relative to L13. Values are rounded to the nearest half-integer.....	66
Table 3: Transformation of halo(alkali)philic <i>Archaea</i> with pRo-5.....	72
Table 4: Different IR-L sequences and their ability for recombination .....	76

---

## 5. References

- Arnold, H.P., Ziese, U., and Zillig, W. (2000) SNDV, a novel virus of the extremely thermophilic and acidophilic archaeon *Sulfolobus*. *Virology* 272: 409-416.
- Baliga, N.S., Bonneau, R., Facciotti, M.T., Pan, M., Glusman, G., Deutsch, E.W., Shannon, P., Chiu, Y., Wenig, R.S., Gan, R.R., Hung, P., Date, S.V., Marcotte, E., Hood, L. and Ng, W.V. (2004) Genome sequence of *Haloarcula marismortui*: A halophilic archaeon from the Dead Sea. *Genome Res* 14: 2221-2234.
- Barns, S.M., Delwicke, C.F., Palmer, J.D., and Pace, N.R. (1996) Perspectives on archaeal diversity, thermophily and monophyly from environmental rRNA sequences. *Proc Natl Acad Sci USA* 93: 9188-9193.
- Brown, J.R. and Doolittle, W.F. (1997) *Archaea* and the prokaryote to eukaryote transition. *Microbiol Mol Biol* 61:456-502.
- Bettstetter, M., Peng, X., Garrett, R.A. and Prangishvili, D. (2003) AFV1, a novel virus infecting hyperthermophilic archaea of the genus *Acidanus*. *Virology* 315: 68-79
- Bamford, D.H., Grimes, J.M., and Stuart, D.I. (2005) What does structure tell us about virus Evolution? *Curr Opin Struct Biol* 15: 655-663.
- Charlebois, R.L., Lam, W.L., Cline, S.W., and Doolittle, W.F. (1987) Characterization of pHV2 from *Hbt. volcanii* and its use in demonstrating transformation of an archaeobacterium, *Proc Natl Acad Sci USA* 84: 8530-8534.
- Cline, S.W. and Doolittle, W.F. (1987) Efficient transfection of the archaeobacterium *Halobacterium halobium*. *J Bacteriol* 169: 1341-1344.
- Del Solar, G., Giraldo, R., Ruiz-Echevarría, M.J., Espinosa, M. and Díaz-Orejas, R. (1998) Replication and control of circular bacterial plasmids. *Microbiol Mol Bio Rev* 62: 434-464
- Dyall-Smith, M., Tang, S.L. and Bath, C. (2003) Haloarchaeal viruses: how diverse are they? *Res Microbiol* 154: 309-313.

- 
- Engelhardt, H. (2007a) Mechanism of osmoprotection by archaeal S-layers: A theoretical study. *J Struct Biol* 160: 190-199.
- Engelhardt, H. (2007b) Are S-layers exoskeletons? The basic function of protein surface layers revisited. *J Struct Biol* 160: 115-124.
- Fauquet, C.M., Mayo, M.A., Maniloff, J., Desselberger, U. and Ball, L.A. (ed.) (2005) *Virus Taxonomy: Classification and Nomenclature of Viruses. Elsevier, Amsterdam*
- Forterre, P. (2006) The origin of viruses and their possible roles in major evolutionary transitions. *Virus Res* 117: 5-16.
- Grant, W.D., and Larsen, H. (1989) Extremely halophilic archaeobacteria. Order Halobacteriales red. nov. In *Bergey's manual of systematic bacteriology*. Pfenning, N. (ed.) The Williams & Wilkins Co., Baltimore, MD, pp 2216-2233.
- Groth, A.C. and Calos, M.P. (2004) Phage integrases: biology and applications. *J Mol Biol* 335: 667-678.
- Guo, F., Gopaul, D.N. and van Duynne, G.D. (1997) Structure of Cre recombinase complexed with DNA in a site-specific recombination synapse. *Nature* 389: 40-46.
- Guzman, L.M., Belin, D., Carson, M.J. and Beckwith, J. (1995) Tight regulation, modulation, and high-level expression by vectors containing the arabinose pBAD promoter. *J Bacteriol* 177: 4121-4130
- Hallet, B., and Sherratt, D.J. (1997) Transposition and site-specific recombination: adapting DNA cut-and-paste mechanisms to a variety of genetic rearrangements. *FEMS Microbiol Rev* 21: 157-178.
- Haring, M., Rachel, R., Peng, X., Garrett, R.A. and Prangishvili, D. (2005) Viral diversity in hot springs of Pozzuoli, Italy, and characterization of a unique archaeal virus, Acidanus bottle-shaped virus, from a new family, the *Ampullaviridae*. *J Virol* 79: 9904-9910.
- Hendrix, R.W., Smith, M.C., Burns, R.N., Ford, M.E., and Hatfull, G.F. (1999) Evolutionary relationships among diverse bacteriophages and prophages: all the world's a phage. *Proc Natl Acad Sci USA* 96: 2192-2197.

- 
- Hendrix, R.W., Lawrence, J.G., Hatfull, G.F., Casjens, S. (2000) The origins and ongoing evolution of viruses. *Trends Microbiol* 8: 504-508.
- Hiestand-Nauer; R. and Iida, S. (1983) Sequence of the site-specific recombinase gene *cin* and of its substrates serving in the inversion of the C segment of bacteriophage P1. *EMBO* 2: 1733-1740.
- Holmes, M.L., Nuttall, S.D. and Dyall-Smith, M.L. (1991) Construction and use of halobacterial shuttle vectors and further studies on *Haloflex* DNA gyrase. *J Bacteriol* 173: 3807-3813
- Holmes, M.L. and Dyall-Smith, M.L. (2000) Sequence and expression of a halobacterial  $\beta$ -galactosidase gene. *Mol Microbiol* 36: 114-122
- Iro, M., Klein, R., Gálos, B., Baranyi, U., Rössler, N. and Witte, A. (2006) The lysogenic region of virus  $\phi$ Ch1: identification of a repressor-operator system and determination of its activity in halophilic Archaea. *Extremophiles* 11: 383-396.
- Iro, M., Ladurner, A., Meissner, C., Derntl, C., Roessler, N., Klein, R., Baranyi, U., Scholz, H., Witte, A. (in prep) Transformation of *Natrialba magadii*: use of  $\phi$ Ch1 elements for a shuttle vector system in haloalkaliphilic Archaea
- Janekovic, D., Wunderl, S., Holz, I., Zillig, W., Gierl, A. and Neumann, H. (1983) TTV1, TTV2, TTV3, a family of viruses of the extremely thermophilic, anaerobic sulfur-reducing archaeobacterium *Thermoproteus tenax*. *Mol Gen Genet* 162: 39-45.
- Jolley, K.A., Russell, R.J.M., Hough, D.W. and Danson, M.J. (1997) Site-directed mutagenesis and halophilicity of dihydrolipoamide dehydrogenase from the halophilic archaeon, *Haloflex volcanii*. *Eur J Biochem* 248: 362-368.
- Jolley, K.A., Rapaport, E., Hough, D.W., Danson, N.J., Woods, W.g. and Dyall-Smith, M.L. (1996) Dihydrolipoamide dehydrogenase from the halophilic archaeon *Haloflex volcanii*: homologous overexpression of the cloned gene. *J Bacteriol* 178: 3044-3048.
- Kamekura, M., Dyall-Smith, M.L., Upasani, V., Ventosa, A., and Kates, M. (1997) Diversity of Alkaliphilic Halobacteria: Proposals for Transfer of *Natronobacterium vacuolatum*, *Natronobacterium magadii*, and *Natronobacterium pharaonis* to *Halorubrum*, *Natrialba*, and *Natronomonas*

- 
- gen. nov., respectively, as *Halorubrum vacuolatum* comb. nov., *Natrialba magadii* comb. nov., and *Natronomonas pharaonis* comb. nov., respectively. *Int J Syst Bacteriol* 47: 853-857.
- Klein, R., Baranyi, U., Rössler, N., Greineder, B., and Witte, A. (2002) *Natrialba magadii* virus  $\phi$ Ch1: first complete nucleotide sequence and functional organization of a virus infecting a haloalkaliphilic archaeon. *Mol Microbiol* 45: 851-863.
- Kornberg, A., and T. A. Baker (1992) DNA replication. W.H. Freeman & Co., New York.
- Luo, Y., Pfister, P., Leisinger, T. and Wasserfallen, A. (2001) The genome of archaeal prophage  $\psi$ M100 encodes the lytic enzyme responsible for autolysis of *Methanothermobacter wolfeii*. *J Bacteriol* 183: 5788-5792.
- Madern, D., Pfister, C., and Zaccai, G. (1995) Mutation at an single amino acid enhances the halophilic behaviour of malate dehydrogenase from *Haloarcula marismortui* in physiological salts. *Eur J Biochem* 230: 1088-1095.
- Meissner, C. (2008) Characterisation of Int2 and determination the binding sites of proteins gp43 and gp44. Diploma thesis, University of Vienna.
- Muskhelishvili, G., Palm, P. and Zillig, W. (1993) SSV1-encoded site-specific recombination system in *Sulfolobus shibatae*. *Mol Gen Genet* 237: 334-342.
- Mengele, R., and Sumper, M. (1992) Drastic differences in glycosylation of related S-layer glycoproteins from moderate and extreme halophiles. *J Biol Chem* 267: 8182-8185.
- Nunes-Düby, S.E., Kwon, H.J., Tirumalai, R.S., Ellenberger, T. and Landy A. (1998) Similarities and differences among 105 members of the Int family of site-specific recombinases. *Nucleic Acids Res* 26: 391-406.
- Ng, W.L. and DasSarma, S. (1993) Minimal replication origin of the 200-kilobase *Halobacterium* plasmid pNRC100. *J Bacteriol* 175: 4584-4596.
- Oren, A., Bratbak, G. and Haldal, M. (1997) Occurrence of virus-like particles in the Dead Sea. *Extremophiles* 1: 143-149.
- Pedulla, M.L. (2003) Origins of highly mosaic mycobacteriophage genomes. *Cell* 113: 171-182.

- 
- Pfeifer, F. and Ghahraman, P. (1993) Plasmid pHH1 of *Halobacterium salinarium*: characterization of the replicon region, the gas vesicle gene cluster and insertion elements. *Mol Gen Genet* 238: 193-200.
- Pfister, P., Wasserfallen, A., Stettler, R., and Leisinger, T. (1998) Molecular analysis of *Methanobacterium* phage  $\psi$ M2. *Mol Microbiol* 30: 233-244.
- Plasterk, R.H., Vrieling, H., and Van de Putte, P. (1983) Transcription initiation of Mu mom depends on methylation of the promoter region and a phage-coded transactivator. *Nature* 27:344-347.
- Prangishvili, D., Vestergaard, G., Häring, M., Aramayo, R., Basta, T., Rachel, R. and Garrett, R.A. (2006) Structural and genomic properties of the hyperthermophilic archaeal virus ATV with an extracellular stage of the reproductive cycle. *J Mol Biol* 359: 1203-1216
- Prangishvili, D., Forterre, P., and Garrett, R.A. (2006) Viruses of the Archaea: A unifying view. *Nature rev Microbiol* 4: 837-848.
- Prangishvili, D. (2003) Evolutionary insights from studies of hyperthermophilic archaea. *Res Microbiol* 154: 289-294.
- Rachel, R., Bettstetter, M., Hedlund, B.P., Haring, M., Kessler, A., Stetter, K.O., and Prangishvili, D. (2002) Remarkable morphological diversity of viruses and virus-like particles in hot terrestrial environments. *Arch Virol* 147: 2419-2429.
- Rawlings, D.E. and Tietze, E. (2001) Comparative biology of IncQ and IncQ-like plasmids. *Microbiol Mol Bio Rev* 65: 481-496.
- Rice, G., Stedman, K., Snyder, J., Wiedenheft, B., Willits, D., Brumfield, S., McDermott, T., and Young, M.J. (2002) Viruses from extreme thermal environments. *Proc Natl Acad Sci USA* 98: 13341-13345.
- Rössler, N., Klein, R., Scholz, H., and Witte, A. (2004) Inversion within the haloalkaliphilic virus  $\phi$ Ch1 results in differential expression of structural proteins. *Mol Microbiol* 52: 413-426.
- Rössler, N., Kögl, K., Hofstätter, H., Iro, M., Scholz, H., Klein, R. and A. Witte. (in prep) ORF34 encodes the tail fibre protein of virus  $\phi$ Ch1.
- Sadowski, P. (1986) Site-specific recombinases: changing partners and doing the twist. *J Bacteriol* 165: 341-347.

- 
- Satyanarayana, T., Raghukumar, C., Shivaji, S. (2005) Extremophilic microbes: Diversity and perspectives. *Curr Sci* 89: 78-90.
- Schnabel, H., Palm, P., Dick, K., and Grampp, B. (1984) Sequence analysis of the insertion element ISH1.8 and of associated structural changes in the genome of phage phiH of the archaeobacterium *Halobacterium halobium*. *EMBO J* 3: 1717-1722.
- Schnabel, H., Palm, P., Dick, K., and Grampp, B. (1982a) *Halobacterium halobium* phage phiH. *EMBO J* 1: 87-92
- Schnabel, H., Schramm, E., Schnabel, R., and Zillig, W. (1982b) Structural variability in the genome of phage phiH of *Halobacterium halobium*. *Mol Gen Genet* 188: 370-377.
- Schnos, M., Zahn, K., Inman, R. B. and Blattner, F. R. (1988) Initiation protein induced helix destabilization at the  $\lambda$  origin: a prepriming step in DNA replication. *Cell* 52:385-395.
- Sleytr, U.B. and Beveridge, T.J. (1999) Bacterial S-layers. *Trends Microbiol* 7: 253-259.
- Stedman, K.M., She, Q., Phan, H., Arnold, H.P., Holz, I., Garrett, R.A. and Zillig, W. (2003) Relationship between fuselloviruses infecting the extremely thermophilic archaeon *Sulfolobus*: SSV1 and SSV2. *Res Microbiol* 154: 259-302
- Stolt, P. and Zillig, W. (1994) Gene regulation in Halophage phiH; more than promoters. *System Appl Microbiol* 16: 591-596.
- Soppa, J. (1999) Normalized nucleotide frequencies allow the definition of archaeal promoter elements for different archaeal groups and reveal base-specific TFB contacts upstream of the TATA box. *Mol Microbiol* 31: 1589-1592.
- Tang, S.L., Fisher, C., Ngui, K., Nuttall, S.D. and Dyall-Smith, M.L. (2002) HF2: a double-stranded DNA tailed haloarchaeal virus with a mosaic genome. *Mol Microbiol* 44: 283-296.
- Tindall, B.J., Mills, A.A. and Grant, W.D. (1980) An alkalophilic red halophilic bacterium with low magnesium requirement from a Kenya soda lake. *J Gen Microbiol* 116: 257-260.



- 
- Tindall, B.J., Ross, H.N.M., and Grant, W.D. (1984) *Natronobacterium* gen. nov. and *Natronococcus* gen. nov., two new genera of haloalkaliphilic archaeobacteria. *Sys Appl Microbiol* 5: 41-57.
- Tomlinson, G.A. and Hochstein, L.I. (1976) *Halobacterium saccharovorum* sp. nov., a carbohydrate-metabolizing, extremely halophilic bacterium. *Can J Microbiol* 22: 587-591
- Torsvik, T., and Dundas, I.D. (1974) Bacteriophage of *Halobacterium salinarium*. *Nature* 248: 680-681.
- Wais, A.C., Kon, M., MacDonald, R.E., and Stollar, B.D. (1975) Salt-dependent bacteriophage infecting *Halobacterium cutirubrum* and *Halobacterium halobium*. *Nature* 256: 314-315.
- Wilson, K.P., Shewchuk, L.M., Brennan, R.G., Otsuk, A.J., Matthews, B.W. (1992) *Escherichia coli* biotin holoenzyme synthetase / bio repressor crystal structure delineates the biotin- and DNA-binding domains. *Proc Natl Acad Sci USA* 89: 9257-9261.
- Witte, A., Baranyi, U., Klein, R., Sulzner, M., Cheng, L., Wanner, G., Krüger, D.H., and Lubitz, W. (1997) Characterization of *Natronobacterium magadii* phage  $\phi$ Ch1, a unique archaeal phage containing DNA and RNA. *Mol Microbiol* 23: 603-616.
- Woese, C.R. and Fox, G.E. (1977) Phylogenetic structure of the prokaryotic domain: the primary kingdoms. *Proc Natl Acad Sci USA* 74: 5088-5090.
- Woese, C.R., Kandler, O., and Wheelis, M.L. (1990) Towards a natural system of organisms: proposal for the domains *Archaea*, *Bacteria*, and *Eucarya*. *Proc Natl Acad Sci USA* 87: 4576-4579.
- Yanisch-Perron, C., Viera, J. and Messing, J. (1985) Improved M13 phage cloning vectors and host strains: nucleotide sequences of the M13mp18 and pUC19 vectors *Gene* 33: 103-119
- Zieg, J., Silverman, M., Hilmen, M., and Simon, M. (1977) Recombinational switch for gene expression. *Science* 196: 170-172.

---

## ***Acknowledgements***

I would like to thank everybody who supported me during my studies and made this thesis possible.

Especially I like to thank Dr. Angela Witte for giving me the opportunity to work on this exciting topic and for all the interesting discussions and the patience when I had a problem. I have learnt much about scientific work.

Furthermore I want to thank my colleagues Richard Dobetsberger, Christina Meissner, Christian Derntl, Michael Reiter and Flora Haider for their help and the nice working environment.

Not at least I want to thank my parents, my brother Christian and my sister Corinna, Kyrill and all my friends for all the support they gave me.

---

## **Zusammenfassung**

Diese Diplomarbeit beschäftigt sich mit dem haloalkaliphilen Archaeon *Nab. magadii* und seinem temperenten Phagen  $\phi$ Ch1.

Der erste Teil der Arbeit konzentriert sich auf die Etablierung eines Transformationssystems für haloalkaliphile Archaea wie *Nab. magadii*.

Bis zum jetzigen Zeitpunkt wurden bakterielle und haloarchaeale Modellsysteme zur Untersuchung von  $\phi$ Ch1 und *Nab. magadii* verwendet. Durch ein Transformationssystem können Experimente auch im natürlichen System durchgeführt werden, was zu einem besseren Verständnis dieser Organismen führt.

Einige Shuttle-Vektoren zwischen *Nab. magadii* und *E. coli* wurden ausgehend vom Genom und im Besonderen vom mutmaßlichen Replikationsursprung des Phagen  $\phi$ Ch1 konstruiert. Anhand der Transformation dieser Vektoren in *Nab. magadii* konnte der Replikationsursprung genauer untersucht werden. Dabei wurde bestätigt, dass die offenen Leserahmen 49 und 55 des  $\phi$ Ch1 Genoms als Repressoren fungieren und eine wichtige Rolle in der Regulation der Virusentwicklung spielen. Um eine mögliche Interaktion dieser Repressoren zu vermeiden, wurde der Vektor pRo-5, der diese Regionen nicht enthält, für weitere Experimente verwendet.

Im Folgenden wurde das pRo-5 Shuttle-Vektor System charakterisiert. Das Plasmid ist stabil in *Nab. magadii* und scheint nicht ins Genom zu integrieren. Das Wirtsspektrum dieses Systems ist des Weiteren nicht auf *Nab. magadii* begrenzt, da einige verschiedene halophile und haloalkaliphile Archaea transformiert werden konnten.

Der zweite Teil der Arbeit beschäftigt sich mit dem Infektionsprozess des Phagen  $\phi$ Ch1. Ein möglicher Einfluss von Int1, einer Integrase der  $\lambda$ -Familie, auf die Variation der „Tail-fibre“ Proteine, die von ORF34 und ORF36 kodiert werden, wurde untersucht. Das *int1* Gen wird von diesen zwei offenen Leserahmen flankiert, die mehrere Wiederholungen von invertierten Sequenzen beinhalten. Es

---

konnte gezeigt werden, dass Int1 für eine Inversion in dieser Region verantwortlich ist, die zum Austausch der C-terminalen Teile von ORF34 und ORF36 führt. Diese Inversionsreaktion ermöglicht ein Andocken des Phagen an spezielle Strukturen der Wirtszelle und ist daher essentiell für eine Infektion.

---

## **Abstract**

This thesis deals with the haloalkaliphilic archaeon *Nab. magadii* and its temperate phage  $\phi$ Ch1.

The first part of this work concentrates on the establishment of a transformation system for haloalkaliphilic Archaea like *Nab. magadii*.

Until now bacterial and haloarchaeal model systems were used to investigate  $\phi$ Ch1 and *Nab. magadii*. With the establishment of a transformation system experiments can be performed in the natural environment, leading to a better insight in these organisms.

Several shuttle-vectors between *Nab. magadii* and *E. coli* were constructed, based on the genome and in particular on the putative origin of replication of the phage  $\phi$ Ch1. The transformation of these vectors into *Nab. magadii* allowed a detailed investigation of the components of the replication origin. This leads to the confirmation that the open reading frames 49 and 55 of the  $\phi$ Ch1 genome act as repressors and carry out an important role in the regulation of virus development. To avoid a possible interaction of these repressors, the vector pRo-5, that lacks these regions, was used for further studies.

In the following the pRo-5 shuttle vector system was characterized. The plasmid was quite stable in *Nab. magadii* and seems not to integrate into the genome. In addition the host range of this system is not limited to *Nab. magadii* as several different halophilic and haloalkaliphilic Archaea were successfully transformed.

The second part of this thesis deals with the infection process of the phage  $\phi$ Ch1. A possible influence of the  $\lambda$ -like integrase Int1 on the variation of the tail fibre proteins ORF34 and ORF36 was investigated. The *int1* gene is flanked by these two open reading frames which contain multiple inverted repeat sequences. It could be shown that Int1 is responsible for an inversion in this region that leads to the exchange of the C-terminal parts of ORF34 and ORF36. This inversion reaction allows the docking of the phage on special structures of the host cell and is therefore essential for an infection.



---

## Curriculum vitae

### Personal details:

*Name:* Angela Ladurner  
*Address:* Staudingergasse 5/13, 1200 Vienna  
*Date and place of birth:* January 29, 1984 in Bregenz, Austria  
*Nationality:* Austria  
*Marital status:* unmarried

### Education:

#### *Completed Education:*

1990-1994 Volksschule Mähdle Wolfurt  
1994-2002 Bundesgymnasium Bregenz Blumenstrasse  
June 2002 Matura (passed with distinction)

#### *Current Education:*

Since 10/2002 Study of Molecular Biology; University of Vienna  
First partial diploma completed in April, 2006  
Since 01/2007 Diploma Thesis at the Department of Microbiology and Immunology (Dr. A. Witte) with the title:  
"Characterization of the inversion reaction of  $\phi$ Ch1 and the establishment of a transformation system for *Natrialba magadii*"

### Working experience:

07/1999 and 07/2000 Alpla Werke Alwin Lehner GmbH & Co KG A-6971 Hard;  
work as office assistant  
07/2001 and 08/2002 Soplar s.a. CH-9450 Altstätten; work as technical assistant  
2004, 2005 and 2006 BA-CA Kunstforum A-1010 Wien, work as museum attendant  
07/2006 Practicum at the Universität des Saarlandes, in the working group of Prof. Elmar Heinzle within the project "Metabolic and Genetic Engineering von *Corynebacterium glutamicum* zur Produktion von L-Methionin"

---

05/2007, 12/2007, 05/2008 Department for Microbiology and Genetics, University of Vienna; work as tutor (supervision of students)

06/2007, 02/2008, 06/2008 FH Campus Vienna Molecular Biotechnology, work as tutor (supervision of students)